# Dual Event-Triggered Polynomial Dynamic Output Control for Positive Fuzzy Systems via an IT2 Membership Function Relaxation Method

Xiaoxiao Wang, Zhiyong Bao, *Member, IEEE*, Xiaomiao Li, *Member, IEEE*, Hak-Keung Lam, *Fellow, IEEE*, Ziwei Wang, *Member, IEEE*

***Abstract*—The co-design problem of dual event-triggered (DET) mechanism and polynomial dynamic output-feedback (PDOF) controller is investigated for positive polynomial fuzzy systems (PPFSs) with uncertainty and disturbance constraints. Specifically, a 1-norm DET mechanism compatible with the positivity of PPFSs is proposed to asynchronously update measurement outputs and PDOF control signals. However, synthesizing this DET-PDOF controller proves challenging due to the coupling of multiple unknown PDOF controller gain matrices within the positivity and stability conditions, which results in complex nonconvex terms. By introducing auxiliary variables and constraints, sufficient conditions for DET-PDOF controller solution are given to ensure both the $L_1$-gain performance and strict positivity of PPFSs with uncertainty and disturbance. Moreover, existing stability analysis results that ignore membership functions (MFs) tend to be conservative, implying that the obtained DET-PDOF controller is effective only within a limited triggered threshold range, leading to worse transmission performance. Therefore, a multivariate optimization method based on an improved genetic algorithm (IGA), which accounts for the system states and PDOF controller variables, is developed to substantially expand the admissible DET threshold range while effectively suppressing dual-triggering frequencies. Finally, a numerical example and a two-linked tank system with parameter uncertainty are provided to validate the feasibility of the proposed scheme.**

***Index Terms*—Positive polynomial fuzzy systems, polynomial dynamic output-feedback (PDOF) control, dual event-triggered (DET), improved genetic algorithm (IGA).**

## I. Introduction

POSITIVE systems are dynamical systems whose state and output variables are restricted to the nonnegative quadrant [1], [2]. The inherent positivity can more appropriately describe practical applications in industrial engineering and biomedical fields, such as pharmacokinetics and biomedicine [3]–[5]. The analysis and control of positive systems are more challenging due to their dynamics being constrained to the nonnegative quadrant, which makes many conventional methods for analyzing general systems less effective. Metzler matrix theory and linear copositive Lyapunov function (LCLF) in [6] provide effective tools for the stability analysis and control synthesis of positive systems, and have been extended to broader fields, including positive singular systems [7], positive Markov jump systems [8], and positive switched systems [9].

Considering the widespread nonlinearity and positivity, the T-S fuzzy model is broadly used in the control synthesis of nonlinear systems due to its approximation ability [10], [11]. Recently, the polynomial fuzzy model (PFM) has emerged as a powerful alternative to conventional T-S fuzzy models, circumventing their restriction to local positive nonlinear system (PNS) representation and complex modeling rules [12], [13]. Although extensive PFM results exist in the literature for PNS, such as state estimation and stabilization [14], [15], the majority of PFMs are constructed using type-1 fuzzy sets, whose deterministic grades of membership lack the adaptability to handle the varying parameter uncertainties inherent in practical systems. To address this limitation, a new class of Interval Type-2 (IT2) fuzzy sets is introduced [16], where the primary membership grades form a footprint of uncertainty (FOU) to capture parameter uncertainties, and the secondary membership grades are invariably one [17], [18]. Recent research has focused on the design of IT2 polynomial state-feedback controller and IT2 polynomial static output-feedback controller in PPFSs [19].

In practice, not all state information of PPFSs can be accurately measured, output-feedback control proves to be more effective than state-feedback control [20]–[23]. While static output-feedback frameworks for PPFSs have been established in [24], [25], dynamic output-feedback (DOF) control can achieve enhanced performance due to its superior capability in handling complex dynamics through internal state compensation. Given this, some DOF results with research difficulty and practical value have been applied in PNS, such as [26], [27]. It can be found that the proposed DOF controller needs to receive output information continuously, ignoring the excessive occupation of limited communication resources by information transmission. In [28]–[30], an event-triggered scheme is designed for the communication channel from the sensor to the DOF controller to reduce communication energy consumption.

This work was funded by Science and Technology Project of Hebei Education Department under Project QN2025118, the Natural Science Foundation under Project (62103356, 62503412) and the Science and Technology Foundation of Qinhuangdao, 202301A295. *(Corresponding Author: Zhiyong Bao)*

Xiaoxiao Wang and Xiaomiao Li are with the Key Lab of Industrial Computer Control Engineering of Hebei Province, Department of Electrical Engineering, Yanshan University, Qinhuangdao 066004, China. (e-mail: wxx19980401@163.com; xsm760595299@163.com).

Zhiyong Bao is with the Measurement Technol and Instrumentat Key Lab Hebei Province, Department of Electrical Engineering, Yanshan University, Qinhuangdao 066004, China. (e-mail: yanshanbzy@163.com).

H.K. Lam is with the Department of Engineering, King's College London, Strand, London WC2R 2LS, United Kingdom. (e-mail: hak-keung.lam@kcl.ac.uk).

Ziwei Wang with the School of Engineering, Lancaster University, LA14YW Lancaster, U.K. (e-mail: z.wang82@lancaster.ac.uk).

In particular, a novel separation design framework is developed in [31] for dynamic event-triggered output feedback control, which employs dual-channel triggering mechanisms to address limited network resources in networked control systems. A critical limitation of the above works is that the standard 2-norm event-triggered mechanism [32]–[34] are incompatible with the analysis framework of positive systems, which typically relies on LCLF. Although [8] initiated the exploration of the DET-DOF control problem for positive linear systems via a 1-norm scheme suitable for positivity analysis, extending this result to PPFSs is challenging due to the complex polynomial structures in the fuzzy subsystems. Furthermore, the different gain parameters in the PDOF control law affect the system's positivity and stability, introducing more nonconvex terms and inevitably increasing the difficulty of solving the convexity problem. To the best of the author's knowledge, the DET-PDOF control for PNS under nonconvex constraints remains unsolved, which inspires the current study.

Most existing studies on event-triggered control for fuzzy systems rely on the membership-function-independent (MFI) method, which accommodates MFs of arbitrary shapes and yields conservative results. This conservative results often restrict the event-triggered threshold to a small range to ensure system stability. However, such a small threshold leads to frequent communications, undermining the primary advantage of event-triggered control. In [19], the IT2 membership-function-dependent (MFD) method is employed to incorporate MF information into stability conditions, thereby enhancing the $L_1$ performance index of fuzzy event-triggered filter. An event-triggered fault-tolerant control strategy based on the MFD method is developed in [35] to derive less conservative stability conditions and address the mismatched premise variables induced by the event-triggered mechanism. Nevertheless, the potential of utilizing MF information to expand the allowable triggering threshold range and enhance triggering performance have not been deeply explored. Moreover, the considered MFs in these works depend strictly on single variables. In contrast, multivariable MFD methods offer a mechanism to coordinate the asynchronous state variables between the system and PDOF controller, which is the pivotal mechanism for achieving superior control performance. Consequently, it is crucial to develop novel multivariable MFD techniques that fully utilize IT2-MF information to provide a broader threshold selection domain and enhance event-triggered control performance.

To address these challenges, the combined DET and PDOF control strategy is explored for PPFSs containing uncertainties to improve control performance under the IGA-MFD approach. The main contributions are as follows:

1) In this paper, the PDOF control problem under a DET mechanism is investigated for PPFSs with parameter uncertainties. Unlike the single-channel triggering strategy [19], a more comprehensive DET mechanism is designed to update both measurement output and PDOF controller signals. Crucially, standard 2-norm event-triggered schemes [32]–[34] are not applicable in the positive system framework, as the resulting quadratic terms are incompatible with the linear structure required for LCLF. Therefore, a 1-norm DET mechanism is proposed that naturally aligns with the inherent positivity of PPFSs.
2) To overcome the challenging nonconvexity arising from the coupling of polynomial controller gains, a convexification approach is proposed. In contrast to the existing method in linear systems that achieves solvability via matrix decomposition and linear programming [8], this paper introduces auxiliary matrices and establishes a crucial linear relationship among them to successfully eliminate the coupling of polynomial terms. Thereby, convex conditions guaranteeing system positivity and stability are derived for the PPFSs.
3) The design flexibility of the DET mechanism regarding trigger frequency and threshold selection is explored from the perspective of MFs. In contrast to univariate MFD [19], [36] or MFI [28] methods, the proposed IGA-MFD method employs multivariate IT2-MFs approximation to handle the asynchronous premise variables between the coupled system dynamics and the PDOF controller. Consequently, it provides a significantly larger upper bound for the triggering threshold interval and achieves a lower triggering frequency compared to conventional approaches.

This paper is structured as follows. The preliminaries are presented in Section II. In Section III, the positivity and $L_1$-gain performance stability analysis are shown. The less conservative results based on IGA-MFD method are shown in Section IV. The simulation and comparison results are provided in Section V, followed by a summary of the paper in Section VI.

*Notation*: A polynomial $\mathbf{m}(\mathbf{x})$ is an SOS if it satisfies $\mathbf{m}(\mathbf{x}) = \sum_{i=1}^{p} \mathbf{n}_i(\mathbf{x})^2$, where $p$ is a nonnegative integer. $A^{(f,s)}$ is the $f$th row, $s$th column element of $A$. For a function $w(t)$ that belongs to $L_1[0,\infty)$ with its $L_1$-norm $\|w(t)\|_{L_1} = \int_{t=0}^{\infty} \|w(t)\|_1 < \infty$. The 1-norm $\|\mathbf{x}\|_1$ and $\infty$-norm $\|\mathbf{x}\|_\infty$ are defined as $\|\mathbf{x}\|_1 = \sum_{k=1}^{n} |x_k|$ and $\|\mathbf{x}\|_\infty = \max\{|x_1|, ..., |x_n|\}$ with $\mathbf{x} \in \Re^n$, respectively. $\mathbf{1}_{s\times s}$ is an $s \times s$ dimensional matrix which has elements of 1. Define $\mathbf{1}_s = (1, ..., 1)^T \in \Re^s$ and $\mathbf{1}_s^f = (0, ..., 0, 1, 0, ..., 0)^T \in \Re^s$, which 1 is the $f^{th}$ element of $\mathbf{1}_s^f$. $\underline{i}$ represents $1, 2, ..., i$.

## II. Preliminaries

### A. IT2 Positive Polynomial Fuzzy System

A PNS with disturbance and uncertainty described by the following IT2 positive PFM with $n_p$ plant rules.

Rule $i$ : If $f_1(\mathbf{x}(t))$ is $\tilde{M}_1^i$ and $\cdots$ and $f_\Psi(\mathbf{x}(t))$ is $\tilde{M}_\Psi^i$, then

$$\begin{cases} \dot{\mathbf{x}}(t) = \mathbf{A}_i(\mathbf{x}(t))\mathbf{x}(t) + \mathbf{B}_i(\mathbf{x}(t))\hat{\mathbf{u}}(t_q^u) \\ \qquad\qquad + \mathbf{B}_{wi}(\mathbf{x}(t))\mathbf{w}(t) \quad t \in [t_q^u, t_{q+1}^u] \\ \mathbf{y}(t) = \mathbf{C}_i(\mathbf{x}(t))\mathbf{x}(t) \\ \mathbf{z}(t) = \mathbf{D}_i(\mathbf{x}(t))\mathbf{x}(t) + \mathbf{E}_{wi}(\mathbf{x}(t))\mathbf{w}(t), \end{cases}$$

in which $\mathbf{x}(t) \in \Re^n$, $\hat{\mathbf{u}}(t_q^u) \in \Re^m$, $\mathbf{w}(t) \in \Re_+^r$, $\mathbf{y}(t) \in \Re^l$ and $\mathbf{z}(t) \in \Re^q$ are the system state, the last transmitted value of the control input $\hat{\mathbf{u}}(t)$, disturbance input, measurement and control output, respectively; $\tilde{M}_\alpha^i$ is an IT2 fuzzy set based on the premise variable $f_\alpha(\mathbf{x}(t))$ of rule $i$, $i = 1, ..., n_p$, $\alpha = 1, \ldots, \Psi$, $\Psi$ is a positive integer; $\mathbf{A}_i(\mathbf{x}(t)) \in \Re^{n\times n}$,

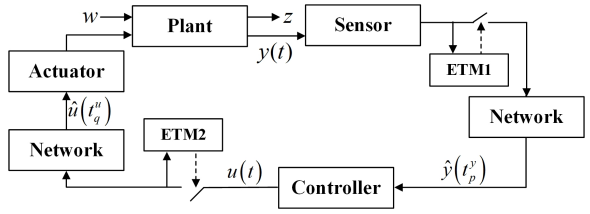


Fig. 1. Block diagram of the dual event-triggered control.

$\mathbf{B}_i(\mathbf{x}(t)) \in \Re^{n\times m}$, $\mathbf{B}_{wi}(\mathbf{x}(t)) \in \Re^{n\times r}$, $\mathbf{C}_i(\mathbf{x}(t)) \in \Re^{l\times n}$, $\mathbf{D}_i(\mathbf{x}(t)) \in \Re^{q\times n}$ and $\mathbf{E}_{wi}(\mathbf{x}(t)) \in \Re^{q\times r}$ are matrices with appropriate dimension. The firing strength of the $i^{th}$ rule is given by the following expression:

$$W_i(\mathbf{x}(t)) = \left[\prod_{\alpha=1}^{\Psi} \underline{\mu}_{\tilde{M}_\alpha^i}(f_\alpha(\mathbf{x}(t))), \prod_{\alpha=1}^{\Psi} \bar{\mu}_{\tilde{M}_\alpha^i}(f_\alpha(\mathbf{x}(t)))\right] = [\underline{w}_i(\mathbf{x}(t)), \overline{w}_i(\mathbf{x}(t))], \quad (1)$$

where $\underline{w}_i(\mathbf{x}(t))$ and $\overline{w}_i(\mathbf{x}(t))$ denote the lower and upper grades of membership governed by the upper and lower MFs $\underline{\mu}_{\tilde{M}_\alpha^i}(f_\alpha(\mathbf{x}(t))) \geq 0$ and $\bar{\mu}_{\tilde{M}_\alpha^i}(f_\alpha(\mathbf{x}(t))) \geq 0$, respectively. Furthermore, it exhibits the property that $0 \leq \underline{\mu}_{\tilde{M}_\alpha^i}(f_\alpha(\mathbf{x}(t))) \leq \bar{\mu}_{\tilde{M}_\alpha^i}(f_\alpha(\mathbf{x}(t))) \leq 1$, which leads to $0 \leq \underline{w}_i(\mathbf{x}(t)) \leq \overline{w}_i(\mathbf{x}(t)) \leq 1$ for all $i$. Then, the dynamics of IT2-PFM is described by

$$\begin{cases} \dot{\mathbf{x}}(t) = \sum_{i=1}^{n_p} \tilde{w}_i(\mathbf{x}(t))\big(\mathbf{A}_i(\mathbf{x}(t))\mathbf{x}(t) + \mathbf{B}_i(\mathbf{x}(t))\hat{\mathbf{u}}(t_q^u) \\ \qquad\qquad + \mathbf{B}_{wi}(\mathbf{x}(t))\mathbf{w}(t)\big) \quad t \in [t_q^u, t_{q+1}^u] \\ \mathbf{y}(t) = \sum_{i=1}^{n_p} \tilde{w}_i(\mathbf{x}(t))\mathbf{C}_i(\mathbf{x}(t))\mathbf{x}(t) \\ \mathbf{z}(t) = \sum_{i=1}^{n_p} \tilde{w}_i(\mathbf{x}(t))\big(\mathbf{D}_i(\mathbf{x}(t))\mathbf{x}(t) + \mathbf{E}_{wi}(\mathbf{x}(t))\mathbf{w}(t)\big), \end{cases} \quad (2)$$

where

$$\tilde{w}_i(\mathbf{x}(t)) = \underline{\varepsilon}_i(\mathbf{x}(t))\underline{w}_i(\mathbf{x}(t)) + \bar{\varepsilon}_i(\mathbf{x}(t))\bar{w}_i(\mathbf{x}(t)), \quad (3)$$

$$\sum\nolimits_{i=1}^{n_p} \tilde{w}_i(\mathbf{x}(t)) = 1, \tilde{w}_i(\mathbf{x}(t)) \geq 0, \qquad \forall i, \quad (4)$$

$\underline{\varepsilon}_i(\mathbf{x}(t)) \in [0,1]$ and $\bar{\varepsilon}_i(\mathbf{x}(t)) \in [0,1]$ are nonlinear type reduction functions not necessarily be known but exist, for all $i$, owning the properties $\underline{\varepsilon}_i(\mathbf{x}(t)) + \bar{\varepsilon}_i(\mathbf{x}(t)) = 1$.

*Definition 1 ( [8]):* If all states and outputs of the system are kept $x(t) \geq 0, y(t) \geq 0$ for any non-negative initial conditions, inputs and external disturbances, the system is positive.

*Lemma 1 ( [8]):* If $A_i(x(t))$ is the Metzler matrix and $D_i(x(t)) \geq 0$, $B_{wi}(x(t)) \geq 0$ and $E_{wi}(x(t)) \geq 0$, then the system

$$\begin{cases} \dot{x}(t) = A_i(x(t))x(t) + B_{wi}(x(t))w(t) \\ z(t) = D_i(x(t))x(t) + E_{wi}(x(t))w(t) \end{cases}$$

is positive.

### *B. Dual-event-based IT2 Positive Polynomial Dynamic Output-feedback Controller*

The block diagram of the DET control is depicted in Fig. 1. event-triggered mechanism 1 (ETM1) governs the transmission of output data for the sensor-to-controller (S-C) channel, while ETM2 handles the latest input data sent to the controller, operating asynchronously with ETM1. The triggering sequences of ETM1 and ETM2 are denoted by $\{t_p^y\}$, $p \in \mathbb{Z}$ and $\{t_q^u\}$, $q \in \mathbb{Z}$. A DET-PDOF controller is designed based on the IPM concept [37] as follows:

Rule $j$ : If $g_1(\mathbf{y}_c(t_q^u))$ is $\tilde{N}_1^j$ AND $\cdots$ AND $g_\Omega(\mathbf{y}_c(t_q^u))$ is $\tilde{N}_\Omega^j$, then

$$\begin{cases} \dot{\mathbf{x}}_c(t) = \mathbf{A}_{cij}(\mathbf{x}_c(t))\mathbf{x}_c(t) + \mathbf{B}_{cj}(\mathbf{x}_c(t))\hat{\mathbf{y}}(t_p^y), \quad t \in [t_p^y, t_{p+1}^y] \\ \mathbf{u}(t) = \mathbf{K}_{cj}(\mathbf{x}_c(t))\mathbf{y}_c(t), \\ \mathbf{y}_c(t) = \mathbf{C}_c\mathbf{x}_c(t), \\ \hat{\mathbf{y}}(t_p^y) = \mathbf{y}(t_p^y), \\ \hat{\mathbf{u}}(t_q^u) = \mathbf{u}(t_q^u), \end{cases}$$

in which $\mathbf{x}_c(t)$, $\mathbf{y}_c(t)$ and $\hat{\mathbf{y}}(t_p^y) \in \Re^l$ are the controller state, controller output and the last transmitted value of the output measurement $\mathbf{y}(t)$, respectively. $\tilde{N}_\beta^j$ is an IT2 fuzzy set based on the premise variable $g_\beta(\mathbf{y}_c(t_q^u))$ of rule $j$, $j = 1, ..., n_c$, $\beta = 1, ..., \Omega$; $\mathbf{A}_{cij}(\mathbf{x}_c(t)) \in \Re^{n\times n}$, $\mathbf{B}_{cj}(\mathbf{x}_c(t)) \in \Re^{n\times l}$ and $\mathbf{K}_{cj}(\mathbf{x}_c(t)) \in \Re^{m\times n}$. The firing strength of the $j^{th}$ rule is given as follows:

$$\tilde{m}_j(\mathbf{y}_c(t_q^u)) = \left[\prod_{\beta=1}^{\Omega} \underline{\mu}_{\tilde{N}_\beta^j}(g_\beta(\mathbf{y}_c(t_q^u))), \prod_{\beta=1}^{\Omega} \bar{\mu}_{\tilde{N}_\beta^j}(g_\beta(\mathbf{y}_c(t_q^u)))\right] = \left[\underline{m}_j(\mathbf{y}_c(t_q^u)), \overline{m}_j(\mathbf{y}_c(t_q^u))\right], \quad (5)$$

where $\underline{m}_j(\mathbf{y}_c(t_q^u))$ and $\overline{m}_j(\mathbf{y}_c(t_q^u))$ denote the lower and upper grades of membership governed by the upper and lower MFs $\underline{\mu}_{\tilde{N}_\beta^j}(g_\beta(\mathbf{y}_c(t_q^u))) \geq 0$ and $\bar{\mu}_{\tilde{N}_\beta^j}(g_\beta(\mathbf{y}_c(t_q^u))) \geq 0$, respectively. Furthermore, it exhibits the property that $0 \leq \underline{\mu}_{\tilde{N}_\beta^j}(g_\beta(\mathbf{y}_c(t_q^u))) \leq \bar{\mu}_{\tilde{N}_\beta^j}(g_\beta(\mathbf{y}_c(t_q^u)) \leq 1$, which leads to $0 \leq \underline{m}_j(\mathbf{y}_c(t_q^u)) \leq \overline{m}_j(\mathbf{y}_c(t_q^u)) \leq 1$ for all $j$. Then the IT2 PDOF controller is described by

$$\begin{cases} \dot{\mathbf{x}}_c(t) = \sum_{i=1}^{n_p}\sum_{j=1}^{n_c} \tilde{w}_i(\mathbf{x}(t))\tilde{m}_j(\mathbf{y}_c(t_q^u))(\mathbf{A}_{cij}(\mathbf{x}_c(t)) \\ \qquad \times\mathbf{x}_c(t) + \mathbf{B}_{cj}(\mathbf{x}_c(t))\hat{\mathbf{y}}(t_p^y)), t \in [t_p^y, t_{p+1}^y] \\ \mathbf{u}(t) = \sum_{j=1}^{n_c} \tilde{m}_j(\mathbf{y}_c(t_q^u))\mathbf{K}_{cj}(\mathbf{x}_c(t))\mathbf{y}_c(t), \\ \mathbf{y}_c(t) = \sum_{j=1}^{n_c} \tilde{m}_j(\mathbf{y}_c(t_q^u))\mathbf{C}_c\mathbf{x}_c(t), \\ \hat{\mathbf{y}}(t_p^y) = \mathbf{y}(t_p^y), \\ \hat{\mathbf{u}}(t_q^u) = \mathbf{u}(t_q^u), \end{cases} \quad (6)$$

where

$$\tilde{m}_j(\mathbf{y}_c(t_q^u)) = \frac{\underline{\kappa}_j(\mathbf{y}_c(t_q^u))\underline{m}_j(\mathbf{y}_c(t_q^u)) + \bar{\kappa}_j(\mathbf{y}_c(t_q^u))\overline{m}_j(\mathbf{y}_c(t_q^u))}{\sum_{k=1}^{c}(\underline{\kappa}_j(\mathbf{y}_c(t_q^u))\underline{m}_k(\mathbf{y}_c(t_q^u)) + \bar{\kappa}_j(\mathbf{y}_c(t_q^u))\overline{m}_k(\mathbf{y}_c(t_q^u)))}, \quad (7)$$

$$\sum\nolimits_{j=1}^{n_c} \tilde{m}_j(\mathbf{y}_c(t_q^u)) = 1, \tilde{m}_j(\mathbf{y}_c(t_q^u)) \geq 0, \qquad \forall j, \quad (8)$$

(7) is the type reduction. $\underline{\kappa}_j(\mathbf{y}_c(t_q^u))$ and $\bar{\kappa}_j(\mathbf{y}_c(t_q^u))$ are predefined functions, for all $j$, have properties of $0 \leq \underline{\kappa}_j(\mathbf{y}_c(t_q^u)) \leq 1$, $0 \leq \bar{\kappa}_j(\mathbf{y}_c(t_q^u)) \leq 1$ and $\underline{\kappa}_j(\mathbf{y}_c(t_q^u)) + \bar{\kappa}_j(\mathbf{y}_c(t_q^u)) = 1$.

*Remark 1:* It should be noted that this paper employs the IT2 fuzzy MFs to handle the uncertainties and nonlinear issues present in the system (2). Unlike type-1 fuzzy sets, IT2 fuzzy sets effectively capture parameter uncertainties through their upper and lower MFs (3).

*Remark 2:* In contrast to traditional static output-feedback

control law, this work establishes a more flexible PDOF control law by introducing an internal controller state $\mathbf{x}_c$. Crucially, unlike most existing T-S fuzzy controllers [28] whose gains are restricted to linear variations, the proposed PDOF controller gains vary nonlinearly and smoothly with the controller state $\mathbf{x}_c$. This dynamic adaptability makes it especially suitable for practical applications such as the population model in biomedicine [3], lipoprotein metabolism and potassium ion transfer model in pharmacokinetics [4].

Then, for generating the S-C channel and controller-to-actuator (C-A) channel data transmission instants $\{t_p^y\}$ and $\{t_q^u\}$, the following DET schemes are designed.

In the S-C channel, the 1-norm ETM1 applicable to PPFS is introduced, described as

$$\begin{aligned}&\hat{\mathbf{y}}\left(t_p^y\right)=\mathbf{y}\left(t_p^y\right), \qquad \forall t\in\left[t_p^y,t_{p+1}^y\right)\\&t_{p+1}^y=\inf\left\{t>t_p^y\middle|\,\|\mathbf{e}_y(t)\|_1>k_y\|\mathbf{y}(t)\|_1\right\},\end{aligned}\tag{9}$$

where $\mathbf{e}_y\left(t\right)=\hat{\mathbf{y}}\left(t_p^y\right)-\mathbf{y}\left(t\right)$ is triggering error.

In the C-A channel, the 1-norm ETM2 applicable to PPFS is introduced, described as

$$\begin{aligned}&\hat{\mathbf{u}}\left(t_q^u\right)=\mathbf{u}\left(t_q^u\right), \qquad \forall t\in\left[t_q^u,t_{q+1}^u\right)\\&t_{q+1}^u=\inf\left\{t>t_q^u\middle|\,\|\mathbf{e}_u(t)\|_1>k_u\|\mathbf{u}(t)\|_1\right\},\end{aligned}\tag{10}$$

where $\mathbf{e}_u\left(t\right)=\hat{\mathbf{u}}\left(t_q^u\right)-\mathbf{u}\left(t\right)=\sum_{j=1}^{n_c}\tilde{m}_j(\mathbf{y}_c(t_q^u))\mathbf{K}_{cj}(\mathbf{x}_c(t))\mathbf{C}_c(\mathbf{x}_c(t_q^u)-\mathbf{x}_c(t))$ is triggering error. $k_y,k_u\in[0,1)$ are constant thresholds to be designed. The PDOF controller gains can be synthesized via matrix decomposition into non-negative and non-positive matrices $\mathbf{K}_{cj}(\mathbf{x}_c(t))=\mathbf{K}_{cj}^{+}(\mathbf{x}_c(t))+\mathbf{K}_{cj}^{-}(\mathbf{x}_c(t))$. Then, we can obtain from event-triggered condition (9) and (10) that

$$-k_y\mathbf{1}_{l\times l}\mathbf{y}(t)\le\mathbf{e}_y(t)\le k_y\mathbf{1}_{l\times l}\mathbf{y}(t),\tag{11}$$

$$\begin{aligned}&-k_u\mathbf{1}_{m\times m}\sum_{j=1}^{n_c}\tilde{m}_j(\mathbf{y}_c(t_q^u))\left(\mathbf{K}_{cj}^{+}(\mathbf{x}_c(t))\right.\\&\left.-\mathbf{K}_{cj}^{-}(\mathbf{x}_c(t))\right)\mathbf{y}_c(t)\le\mathbf{e}_u(t)\le k_u\mathbf{1}_{m\times m}\\&\sum_{j=1}^{n_c}\tilde{m}_j(\mathbf{y}_c(t_q^u))\left(\mathbf{K}_{cj}^{+}(\mathbf{x}_c(t))-\mathbf{K}_{cj}^{-}(\mathbf{x}_c(t))\right)\mathbf{y}_c(t).\end{aligned}\tag{12}$$

### C. Dual-event-based Augmented Closed-Loop System

In the following, $\mathbf{x}\left(t\right)$, $\mathbf{x}_c\left(t\right)$ and $\mathbf{y}_c\left(t_q^u\right)$ are represented by $\mathbf{x}$, $\mathbf{x}_c$ and $\hat{\mathbf{y}}_c$ to enhance readability. Denote $\bar{\mathbf{e}}=\mathbf{x}-\mathbf{x}_c$ as the state error, we obtain the augmented PPFSs formed by IT2-PFM (2) and IT2-PDOF controllers (6) as follows:

$$\begin{cases}\dot{\boldsymbol{\chi}}=\sum\limits_{i=1}^{n_p}\sum\limits_{j=1}^{n_c}\tilde{w}_i(\mathbf{x})\tilde{m}_j(\hat{\mathbf{y}}_c)\\\quad\times\left(\boldsymbol{\mathcal{A}}_{ij}(\mathbf{x},\mathbf{x}_c)\boldsymbol{\chi}+\boldsymbol{\mathcal{B}}_{ij}(\mathbf{x},\mathbf{x}_c)\hat{\mathbf{e}}+\boldsymbol{\mathcal{B}}_{wij}(\mathbf{x})\mathbf{w}\right)\\\boldsymbol{z}=\sum\limits_{i=1}^{n_p}\sum\limits_{j=1}^{n_c}\tilde{w}_i(\mathbf{x})\tilde{m}_j(\hat{\mathbf{y}}_c)\left(\boldsymbol{\mathcal{D}}_{ij}(\mathbf{x},\mathbf{x}_c)\boldsymbol{\chi}+\boldsymbol{\mathcal{E}}_{wi}(\mathbf{x})\mathbf{w}\right)\end{cases},\tag{13}$$

where $\boldsymbol{\chi}=\left[\mathbf{x}^T,\bar{\mathbf{e}}^T\right]^T$, $\hat{\mathbf{e}}=\left[\mathbf{e}_y^T,\mathbf{e}_j^{uT}\right]^T$, $\mathbf{e}_u=\sum_{j=1}^{n_c}\tilde{m}_j(\mathbf{y}_c(t_q^u))\mathbf{e}_j^u$, and then

$$\boldsymbol{\mathcal{A}}_{ij}(\mathbf{x},\mathbf{x}_c)=\begin{bmatrix}\boldsymbol{\mathcal{A}}_{ij}^{11}(\mathbf{x},\mathbf{x}_c) & \boldsymbol{\mathcal{A}}_{ij}^{12}(\mathbf{x},\mathbf{x}_c)\\ \boldsymbol{\mathcal{A}}_{ij}^{21}(\mathbf{x},\mathbf{x}_c) & \boldsymbol{\mathcal{A}}_{ij}^{22}(\mathbf{x},\mathbf{x}_c)\end{bmatrix},$$

$$\boldsymbol{\mathcal{B}}_{ij}(\mathbf{x},\mathbf{x}_c)=\begin{bmatrix}\mathbf{0} & \mathbf{B}_i(\mathbf{x})\\ -\mathbf{B}_{cj}(\mathbf{x}_c) & \mathbf{B}_i(\mathbf{x})\end{bmatrix},\boldsymbol{\mathcal{B}}_{wij}(\mathbf{x})=\begin{bmatrix}\mathbf{B}_{wi}(\mathbf{x})\\ \mathbf{B}_{wi}(\mathbf{x})\end{bmatrix},$$

$$\boldsymbol{\mathcal{D}}_{ij}(\mathbf{x},\mathbf{x}_c)=[\,\mathbf{D}_i(\mathbf{x})\;\;\mathbf{0}\,],\boldsymbol{\mathcal{E}}_{wi}(\mathbf{x})=\mathbf{E}_{wi}(\mathbf{x}),$$

with

$$\begin{aligned}\boldsymbol{\mathcal{A}}_{ij}^{11}(\mathbf{x},\mathbf{x}_c)=&\mathbf{A}_i(\mathbf{x})+\mathbf{B}_i(\mathbf{x})\mathbf{K}_{cj}(\mathbf{x}_c)\mathbf{C}_c,\\\boldsymbol{\mathcal{A}}_{ij}^{12}(\mathbf{x},\mathbf{x}_c)=&-\mathbf{B}_i(\mathbf{x})\mathbf{K}_{cj}(\mathbf{x}_c)\mathbf{C}_c,\\\boldsymbol{\mathcal{A}}_{ij}^{21}(\mathbf{x},\mathbf{x}_c)=&\mathbf{A}_i(\mathbf{x})+\mathbf{B}_i(\mathbf{x})\mathbf{K}_{cj}(\mathbf{x}_c)\mathbf{C}_c\\&-\mathbf{A}_{cij}(\mathbf{x}_c)-\mathbf{B}_{cj}(\mathbf{x}_c)\mathbf{C}(\mathbf{x}),\\\boldsymbol{\mathcal{A}}_{ij}^{22}(\mathbf{x},\mathbf{x}_c)=&\mathbf{A}_{cij}(\mathbf{x}_c)-\mathbf{B}_i(\mathbf{x})\mathbf{K}_{cj}(\mathbf{x}_c)\mathbf{C}_c.\end{aligned}$$

## III. Dual-Event-based Polynomial Fuzzy Dynamic Output-Feedback Control for IT2 Positive Polynomial Fuzzy Systems

*Lemma 2:* The system (2) is said to be stable with $L_1$-gain performance if the following conditions hold.

1) The PPFS is positive and asymptotically stable; specifically, for $\mathbf{w}\left(t\right)=0$, $\int_0^\infty\|\boldsymbol{\chi}\left(t\right)\|_1dt<\infty$ holds.
2) The following inequality satisfies
$$\int_{t=0}^{\infty}\|\mathbf{z}\left(t\right)\|_1dt<\gamma\int_{t=0}^{\infty}\|\mathbf{w}\left(t\right)\|_1dt$$
for $\mathbf{w}\left(t\right)\in L_1\left[0,\infty\right)$ and a positive prescribed performance $\gamma$.

### A. $L_1$-Gain Performance Stability for Dual-Event-based Augmented Closed-Loop System

For $\mathbf{w}(t)=0$, a LCLF candidate for PPFSs is constructed to ensure asymptotic stability at $L_1$-gain performance level for dual-event-based augmented closed-loop systems (13).

$$\mathbf{V}(\mathbf{x},\mathbf{x}_c)=\boldsymbol{\xi}^T\boldsymbol{\chi},\tag{14}$$

where $\boldsymbol{\xi}^T=\left[\boldsymbol{\xi}_1{}^T\;\;\boldsymbol{\xi}_2{}^T\right]$, $\boldsymbol{\xi}_1,\boldsymbol{\xi}_2\succ 0$ are constant vectors. According to (11), (12) and $\mathbf{B}_{cj}(\mathbf{x}_c)\ge 0$, then

$$\begin{aligned}&\dot{\mathbf{V}}(\mathbf{x},\mathbf{x}_c)=\boldsymbol{\xi}^T\dot{\boldsymbol{\chi}}\\&=\sum_{i=1}^{n_p}\sum_{j=1}^{n_c}\tilde{w}_i(\mathbf{x})\tilde{m}_j(\hat{\mathbf{y}}_c)\left(\boldsymbol{\xi}^T\boldsymbol{\mathcal{A}}_{ij}(\mathbf{x},\mathbf{x}_c)\boldsymbol{\chi}+\boldsymbol{\xi}^T\boldsymbol{\mathcal{B}}_{ij}(\mathbf{x},\mathbf{x}_c)\hat{\mathbf{e}}\right)\\&\le\sum_{i=1}^{n_p}\sum_{j=1}^{n_c}\tilde{w}_i(\mathbf{x})\tilde{m}_j(\hat{\mathbf{y}}_c)\Bigg\{\left[\;\boldsymbol{\xi}_1{}^T\;\;\boldsymbol{\xi}_2{}^T\right]\begin{bmatrix}\boldsymbol{\mathcal{A}}_{ij}^{11}(\mathbf{x},\mathbf{x}_c) & \boldsymbol{\mathcal{A}}_{ij}^{12}(\mathbf{x},\mathbf{x}_c)\\ \boldsymbol{\mathcal{A}}_{ij}^{21}(\mathbf{x},\mathbf{x}_c) & \boldsymbol{\mathcal{A}}_{ij}^{22}(\mathbf{x},\mathbf{x}_c)\end{bmatrix}\\&\quad\times\begin{bmatrix}\mathbf{x}\\ \bar{\mathbf{e}}\end{bmatrix}+\boldsymbol{\xi}_2{}^T\mathbf{B}_{cj}(\mathbf{x}_c)k_y\mathbf{1}_{l\times l}\mathbf{C}_i(\mathbf{x})\mathbf{x}\\&\quad+(\boldsymbol{\xi}_1{}^T+\boldsymbol{\xi}_2{}^T)\mathbf{B}_i(\mathbf{x})k_u\mathbf{1}_{m\times m}\left(\mathbf{K}_{cj}^{+}(\mathbf{x}_c)-\mathbf{K}_{cj}^{-}(\mathbf{x}_c)\right)\mathbf{C}_c\mathbf{x}_c\Bigg\}\\&=\sum_{i=1}^{n_p}\sum_{j=1}^{n_c}\tilde{w}_i(\mathbf{x})\tilde{m}_j(\hat{\mathbf{y}}_c)\left[\,\boldsymbol{\Xi}_{ij}^1\left(\mathbf{x},\mathbf{x}_c\right)\;\;\boldsymbol{\Xi}_{ij}^2\left(\mathbf{x},\mathbf{x}_c\right)\right]\begin{bmatrix}\mathbf{x}\\ \bar{\mathbf{e}}\end{bmatrix}.\end{aligned}\tag{15}$$

*Remark 3:* Due to the nonnegativity of the system states, the 1-norm used in (9) and (10) is equivalent to the sum of the state variables, such as the size of biological populations, the liquid level and the density of matter in physics, which the 2-norm [32], [33] fails to capture intuitively. From (15), the principal advantage of the 1-norm event-triggered condition

is its linearity [8], and this linearity perfectly aligns with the LCLF framework, significantly facilitating the scaling of state variables.

When $\mathbf{w}(t)=0$ is applied to the system (13), we get

$$\mathbf{z}=\sum_{i=1}^{n_p}\sum_{j=1}^{n_c}\tilde{w}_i(\mathbf{x})\tilde{m}_j(\hat{\mathbf{y}}_c)\boldsymbol{\mathcal{D}}_{ij}(\mathbf{x},\mathbf{x}_c)\boldsymbol{\chi}, \tag{16}$$

it holds that $\boldsymbol{\mathcal{D}}_{ij}(\mathbf{x},\mathbf{x}_c)\geq 0$ because of the positive constraint. So, $\dot{\mathbf{V}}(\mathbf{x},\mathbf{x}_c)\leq 0$ can be guaranteed by follows

$$\begin{aligned}&\left[\begin{array}{cc}\boldsymbol{\Xi}_{ij}^1(\mathbf{x},\mathbf{x}_c) & \boldsymbol{\Xi}_{ij}^2(\mathbf{x},\mathbf{x}_c)\end{array}\right]+\mathbf{1}_q^T\boldsymbol{\mathcal{D}}_{ij}(\mathbf{x},\mathbf{x}_c)\\&=\left[\begin{array}{cc}\hat{\boldsymbol{\Xi}}_{ij}^1(\mathbf{x},\mathbf{x}_c) & \hat{\boldsymbol{\Xi}}_{ij}^2(\mathbf{x},\mathbf{x}_c)\end{array}\right]\leq 0.\end{aligned} \tag{17}$$

Define $\sigma_1\mathbf{1}_{l\times n}\leq\mathbf{C}_c\leq\sigma_2\mathbf{1}_{l\times n}$, $\sigma_2\geq\sigma_1\geq 0$, it follows from (17) that

$$\begin{aligned}\hat{\boldsymbol{\Xi}}_{ij}^1(\mathbf{x},\mathbf{x}_c)\leq&\big(\boldsymbol{\xi}_1{}^T+\boldsymbol{\xi}_2{}^T\big)\mathbf{A}_i(\mathbf{x})-\boldsymbol{\xi}_2{}^T\mathbf{A}_{cij}(\mathbf{x}_c)\\&+\big(\boldsymbol{\xi}_1{}^T+\boldsymbol{\xi}_2{}^T\big)\mathbf{B}_{\max}\sigma_2\big(\mathbf{I}+k_u\mathbf{1}_{m\times m}\big)\mathbf{K}_{cj}^+(\mathbf{x}_c)\mathbf{1}_{l\times n}\\&+\big(\boldsymbol{\xi}_1{}^T+\boldsymbol{\xi}_2{}^T\big)\big(\mathbf{B}_{\min}\sigma_1\mathbf{I}-\mathbf{B}_{\max}k_u\sigma_2\mathbf{1}_{m\times m}\big)\mathbf{K}_{cj}^-(\mathbf{x}_c)\mathbf{1}_{l\times n}\\&-\boldsymbol{\xi}_2{}^T\mathbf{B}_{cj}(\mathbf{x}_c)\big(\mathbf{I}-k_y\mathbf{1}_{l\times l}\big)\mathbf{C}_i(\mathbf{x})+\mathbf{1}_q^T\mathbf{D}_i(\mathbf{x}),\end{aligned} \tag{18}$$

$$\begin{aligned}\hat{\boldsymbol{\Xi}}_{ij}^2(\mathbf{x},\mathbf{x}_c)\leq&\boldsymbol{\xi}_2{}^T\mathbf{A}_{cij}(\mathbf{x}_c)\\&-\big(\boldsymbol{\xi}_1{}^T+\boldsymbol{\xi}_2{}^T\big)\mathbf{B}_{\min}\sigma_1\big(\mathbf{I}+k_u\mathbf{1}_{m\times m}\big)\mathbf{K}_{cj}^+(\mathbf{x}_c)\mathbf{1}_{l\times n}\\&-\big(\boldsymbol{\xi}_1{}^T+\boldsymbol{\xi}_2{}^T\big)\big(\mathbf{B}_{\max}\sigma_2\boldsymbol{I}-\mathbf{B}_{\min}k_u\sigma_1\boldsymbol{I}_{m\times m}\big)\mathbf{K}_{cj}^-(\mathbf{x}_c)\mathbf{1}_{l\times n},\end{aligned} \tag{19}$$

where $\mathbf{B}_{\max}=[b_{fs,max}]\in\mathbb{R}^{n\times m}$ is a matrix whose element in the $f$-th row and $s$-th column is $b_{fs}=\max\limits_{\mathbf{x}\in\mathcal{X}}\{b_{fs,i}(\mathbf{x})\}$, $f=1,...,n, s=1,...,m, i=1,...,n_p$. $\mathbf{B}_{\min}=[b_{fs,min}]$, similarly. Next, the polynomial terms formed by multiplying $\boldsymbol{\xi}_1{}^T+\boldsymbol{\xi}_2{}^T$ by $\mathbf{K}_{cj}^+(\mathbf{x}_c)$ or $\mathbf{K}_{cj}^-(\mathbf{x}_c)$ in (18) and (19) are nonconvex terms that cannot be resolved by the Matlab SOSTOOLS, so we construct the following auxiliary matrices to replace the nonconvex terms.

$$\begin{aligned}\alpha_1\mathbf{O}_{cj}^+(\mathbf{x}_c)\leq&(\boldsymbol{\xi}_1{}^T+\boldsymbol{\xi}_2{}^T)\mathbf{B}_{\min}\mathbf{K}_{cj}^+(\mathbf{x}_c)\\\leq&(\boldsymbol{\xi}_1{}^T+\boldsymbol{\xi}_2{}^T)\mathbf{B}_{\max}\mathbf{K}_{cj}^+(\mathbf{x}_c)=\mathbf{O}_{cj}^+(\mathbf{x}_c),\end{aligned} \tag{20}$$

$$\begin{aligned}\mathbf{O}_{cj}^-(\mathbf{x}_c)=&(\boldsymbol{\xi}_1{}^T+\boldsymbol{\xi}_2{}^T)\mathbf{B}_{\max}\mathbf{K}_{cj}^-(\mathbf{x}_c)\\\leq&(\boldsymbol{\xi}_1{}^T+\boldsymbol{\xi}_2{}^T)\mathbf{B}_{\min}\mathbf{K}_{cj}^-(\mathbf{x}_c)\leq\alpha_2\mathbf{O}_{cj}^-(\mathbf{x}_c),\end{aligned} \tag{21}$$

$$\boldsymbol{\xi}_2{}^T\mathbf{A}_{cij}(\mathbf{x}_c)=\sum\nolimits_{f=1}^{n}\mathbf{m}_f^{cij}(\mathbf{x}_c), \tag{22}$$

$$\boldsymbol{\xi}_2{}^T\mathbf{B}_{cj}(\mathbf{x}_c)=\sum\nolimits_{f=1}^{n}\mathbf{n}_f^{cj}(\mathbf{x}_c), \tag{23}$$

where $0\leq\alpha_1\leq 1, 0\leq\alpha_2\leq 1$.

Then, taking (20), (21), (22) and (23) into (18) and (19), we can summarize as follows

$$\dot{\mathbf{V}}(\mathbf{x},\mathbf{x}_c)\leq\sum_{i=1}^{n_p}\sum_{j=1}^{n_c}\tilde{w}_i(\mathbf{x})\tilde{m}_j(\hat{\mathbf{y}}_c)\Big[\begin{array}{cc}\tilde{\boldsymbol{\Xi}}_{ij}^1(\mathbf{x},\mathbf{x}_c) & \tilde{\boldsymbol{\Xi}}_{ij}^2(\mathbf{x},\mathbf{x}_c)\end{array}\Big]\boldsymbol{\chi},$$

$$\begin{aligned}\tilde{\boldsymbol{\Xi}}_{ij}^1(\mathbf{x},\mathbf{x}_c)=&\big(\boldsymbol{\xi}_1{}^T+\boldsymbol{\xi}_2{}^T\big)\mathbf{A}_i(\mathbf{x})+\mathbf{O}_{cj}^-(\mathbf{x}_c)\big(\alpha_2\sigma_1-mk_u\sigma_2\big)\\&\times\mathbf{1}_{l\times n}+\mathbf{O}_{cj}^+(\mathbf{x}_c)\sigma_2\big(\mathbf{I}+mk_u\mathbf{1}_{l\times l}\big)\mathbf{1}_{l\times n}-\sum_{f=1}^{n}\mathbf{m}_f^{cij}(\mathbf{x}_c)\\&-\sum_{f=1}^{n}\mathbf{n}_f^{cj}(\mathbf{x}_c)\big(\mathbf{I}-k_y\mathbf{1}_{l\times l}\big)\mathbf{C}_i(\mathbf{x})+\mathbf{1}_q^T\mathbf{D}_i(\mathbf{x})\leq-\varepsilon\mathbf{1}_n,\end{aligned} \tag{24}$$

$$\begin{aligned}\tilde{\boldsymbol{\Xi}}_{ij}^2(\mathbf{x},\mathbf{x}_c)=&\sum_{f=1}^{n}\mathbf{m}_f^{cij}(\mathbf{x}_c)-\mathbf{O}_{cj}^+(\mathbf{x}_c)\alpha_1\sigma_1\big(\mathbf{I}+mk_u\mathbf{1}_{l\times l}\big)\\&\times\mathbf{1}_{l\times n}-\mathbf{O}_{cj}^-(\mathbf{x}_c)\big(\sigma_2-mk_u\alpha_2\sigma_1\big)\mathbf{1}_{l\times n}\leq-\varepsilon\mathbf{1}_n,\end{aligned} \tag{25}$$

from (24) and (25), there is a positive constant $\varepsilon$ satisfying $\dot{\mathbf{V}}(\mathbf{x},\mathbf{x}_c)\leq-\varepsilon\|\boldsymbol{\chi}\|_1$, it is easily obtained that $\int_{t=t_0}^{\infty}\|\boldsymbol{\chi}\|_1 dt\leq\infty$. Then, the stability of PPFS (13) can be confirmed.

*Remark 4:* Compared with a commonly used quadratic Lyapunov function, the LCLF fully captures the inherent positivity of positive systems, naturally matches positive state trajectories, and typically yields less conservative results. Furthermore, the 1-norm DET conditions are highly consistent with this type of LCLF, which facilitates the stability analysis of positive systems and the design of triggering controllers.

Next, for the system with $\mathbf{w}(t)\neq 0$, consider the performance index defined as $\mathbf{J}(\mathbf{x},\mathbf{x}_c)=\int_{t=0}^{\infty}(\|\mathbf{z}\|_1-\gamma\|\mathbf{w}\|_1)dt$. Then, we have

$$\begin{aligned}\mathbf{J}(\mathbf{x},\mathbf{x}_c)=&\int_{t=0}^{\infty}\Big(\dot{\mathbf{V}}(\mathbf{x},\mathbf{x}_c)+\|\mathbf{z}\|_1-\gamma\|\mathbf{w}\|_1\Big)dt-\mathbf{V}(\mathbf{x},\mathbf{x}_c)\\=&\sum_{i=1}^{n_p}\sum_{j=1}^{n_c}\tilde{w}_i(\mathbf{x})\tilde{m}_j(\hat{\mathbf{y}}_c)\Big\{\big(\boldsymbol{\xi}^T\mathcal{A}_{ij}(\mathbf{x},\mathbf{x}_c)+\mathbf{1}_q^T\mathcal{D}_{ij}(\mathbf{x},\mathbf{x}_c)\big)\boldsymbol{\chi}\\&+\big(\boldsymbol{\xi}^T\mathcal{B}_{wij}(\mathbf{x})+\mathbf{1}_q^T\mathcal{E}_{wi}(\mathbf{x})-\gamma\mathbf{1}_r^T\big)\mathbf{w}+\boldsymbol{\xi}^T\mathcal{B}_{ij}(\mathbf{x},\mathbf{x}_c)\hat{\mathbf{e}}\Big\}\\&-\mathbf{V}(\mathbf{x},\mathbf{x}_c)\\=&\sum_{i=1}^{n_p}\sum_{j=1}^{n_c}\tilde{w}_i(\mathbf{x})\tilde{m}_j(\hat{\mathbf{y}}_c)\Big(\tilde{\boldsymbol{\Xi}}_{ij}(\mathbf{x},\mathbf{x}_c)\boldsymbol{\chi}+\boldsymbol{\Psi}_i(\mathbf{x})\mathbf{w}\Big)-\mathbf{V}(\mathbf{x},\mathbf{x}_c).\end{aligned} \tag{26}$$

The stability and $L_1$-gain performance of the PPFS (13) are guaranteed if $\boldsymbol{\Psi}_i(\mathbf{x})\leq 0$, which leads to the $L_1$-gain performance condition $\mathbf{J}(\mathbf{x},\mathbf{x}_c)\leq 0$. Then, the PDOF controller design forms in (20), (21), (22) and (23) are provided such that the augmented system (13) is asymptotically stable and satisfies the $L_1$-gain performance.

Next, the SOS-based conditions are derived as follows.

*Theorem 1:* For given positive scalars $\varepsilon$, $\gamma$, $0<k\leq 1$, $0<k_c\leq 1$, $0\leq\alpha_1\leq 1$, $0\leq\alpha_2\leq 1$, vectors $\boldsymbol{\xi}_1,\boldsymbol{\xi}_2\succ 0$, the dual-event-based PPFS (13) is asymptotically stable with $L_1$ performance such that

$$\begin{aligned}&-\Big(\tilde{\boldsymbol{\Xi}}_{ij}^{1,(1,s)}(\mathbf{x},\mathbf{x}_c)+\varepsilon+\nu(\mathbf{x},\mathbf{x}_c)\Big)\text{ is SOS},\\&\qquad i\in\underline{n_p},j\in\underline{n_c},s\in\underline{n}\\&-\Big(\tilde{\boldsymbol{\Xi}}_{ij}^{2,(1,s)}(\mathbf{x},\mathbf{x}_c)+\varepsilon+\nu(\mathbf{x},\mathbf{x}_c)\Big)\text{ is SOS},\\&\qquad i\in\underline{n_p},j\in\underline{n_c},s\in\underline{n}\\&-\Big(\boldsymbol{\Psi}_i^{(1,s)}(\mathbf{x})+\nu(\mathbf{x})\Big)\text{ is SOS},i\in\underline{n_p},s\in\underline{r}\\&-\Big(\mathbf{O}_{-}^{cj,(1,s)}(\mathbf{x}_c)+\nu(\mathbf{x}_c)\Big)\text{ is SOS},j\in\underline{n_c},s\in\underline{l}\\&\mathbf{O}_{+}^{cj,(1,s)}(\mathbf{x}_c)-\nu(\mathbf{x}_c)\text{ is SOS},j\in\underline{n_c},s\in\underline{l}\\&\mathbf{N}_{cj}^{(f,s)}(\mathbf{x}_c)-\nu(\mathbf{x}_c)\text{ is SOS},j\in\underline{n_c},f\in\underline{n},s\in\underline{l}\end{aligned}$$

where $\nu(\mathbf{x})>0$, $\nu(\mathbf{x}_c)>0$ and $\nu(\mathbf{x},\mathbf{x}_c)>0$ are predefined scalar polynomials. $\tilde{\boldsymbol{\Xi}}_{ij}^{m,(1,s)}(\mathbf{x},\mathbf{x}_c)$, $m\in\{1,2\}$, $\boldsymbol{\Psi}_i^{(1,s)}(\mathbf{x})$ are defined in (24), (25) and (26).

$\boldsymbol{\xi}_1 = [\xi_{11}, \xi_{12}, ..., \xi_{1n}]^T \succ 0$, $\boldsymbol{\xi}_2 = [\xi_{21}, \xi_{22}, ..., \xi_{2n}]^T \succ 0$, $\mathbf{O}_{cj}^{+}(\mathbf{x}_c) = \left[o_{+}^{cj,1}(\mathbf{x}_c), o_{+}^{cj,2}(\mathbf{x}_c), ..., o_{+}^{cj,l}(\mathbf{x}_c)\right]$, $\mathbf{O}_{+}^{cj,(1,s)}(\mathbf{x}_c) = o_{+}^{cj,s}(\mathbf{x}_c)$; $\mathbf{M}_{cij}(\mathbf{x}_c) = \left[m_1^{cij}(\mathbf{x}_c), ..., m_f^{cij}(\mathbf{x}_c)\right]^T = \left(m_{fs}^{cij}(\mathbf{x}_c)\right) \in \Re^{n\times n}$ and $\mathbf{N}_{cj}(\mathbf{x}_c) = \left[n_1^{cj}(\mathbf{x}_c), ..., n_f^{cj}(\mathbf{x}_c)\right]^T = \left(n_{fs}^{cj}(\mathbf{x}_c)\right) \in \Re^{n\times l}$, $\mathbf{N}_{cj}^{(f,s)}(\mathbf{x}_c) = n_{fs}^{cj}(\mathbf{x}_c)$, $\forall i \in \underline{n_p}$, $j \in \underline{n_c}$.

### *B. The Positivity for Dual-event-based Augmented Closed-Loop System*

According to DET errors (11), (12) and (13), we can get

$$\dot{\boldsymbol{\chi}} \geq \sum_{i=1}^{n_p}\sum_{j=1}^{n_c} \tilde{w}_i(\mathbf{x})\tilde{m}_j(\hat{\mathbf{y}}_c)\Big(\hat{\boldsymbol{\mathcal{A}}}_{ij}(\mathbf{x},\mathbf{x}_c)\boldsymbol{\chi} + \boldsymbol{\mathcal{B}}_{wij}(\mathbf{x})\mathbf{w}\Big), \quad (27)$$

where

$$\begin{aligned}
\hat{\boldsymbol{\mathcal{A}}}_{ij}^{11}(\mathbf{x},\mathbf{x}_c) =& \mathbf{A}_i(\mathbf{x}) + \mathbf{B}_i(\mathbf{x})\big(\sigma_1\mathbf{I} - k_u\sigma_2\mathbf{1}_{m\times m}\big)\mathbf{K}_{cj}^{+}(\mathbf{x}_c)\mathbf{1}_{l\times n} \\
&+ \mathbf{B}_i(\mathbf{x})\sigma_2\big(\mathbf{I} + k_u\mathbf{1}_{m\times m}\big)\mathbf{K}_{cj}^{-}(\mathbf{x}_c)\mathbf{1}_{l\times n}, \\
\hat{\boldsymbol{\mathcal{A}}}_{ij}^{12}(\mathbf{x},\mathbf{x}_c) =& -\mathbf{B}_i(\mathbf{x})\big(\sigma_2\mathbf{I} - k_u\sigma_1\mathbf{1}_{m\times m}\big)\mathbf{K}_{cj}^{+}(\mathbf{x}_c)\mathbf{1}_{l\times n} \\
&- \mathbf{B}_i(\mathbf{x})\sigma_1\big(\mathbf{I} + k_u\mathbf{1}_{m\times m}\big)\mathbf{K}_{cj}^{-}(\mathbf{x}_c)\mathbf{1}_{l\times n}, \\
\hat{\boldsymbol{\mathcal{A}}}_{ij}^{21}(\mathbf{x},\mathbf{x}_c) =& \mathbf{A}_i(\mathbf{x}) + \mathbf{B}_i(\mathbf{x})\left(\sigma_1\mathbf{I} - k_u\sigma_2\mathbf{1}_{m\times m}\right)\mathbf{K}_{cj}^{+}(\mathbf{x}_c)\mathbf{1}_{l\times n} \\
&+ \mathbf{B}_i(\mathbf{x})\sigma_2\big(\mathbf{I} + k_u\mathbf{1}_{m\times m}\big)\mathbf{K}_{cj}^{-}(\mathbf{x}_c)\mathbf{1}_{l\times n} \\
&- \mathbf{A}_{cij}(\mathbf{x}_c) - \mathbf{B}_{cj}(\mathbf{x}_c)\big(\mathbf{I} + k_y\mathbf{1}_{l\times l}\big)\mathbf{C}_i(\mathbf{x}), \\
\hat{\boldsymbol{\mathcal{A}}}_{ij}^{22}(\mathbf{x},\mathbf{x}_c) =& \mathbf{A}_{cij}(\mathbf{x}_c) - \mathbf{B}_i(\mathbf{x})\big(\sigma_2\mathbf{I} - k_u\sigma_1\mathbf{1}_{m\times m}\big)\mathbf{K}_{cj}^{+}(\mathbf{x}_c)\mathbf{1}_{l\times n} \\
&- \mathbf{B}_i(\mathbf{x})\sigma_1\big(\mathbf{I} + k_u\mathbf{1}_{m\times m}\big)\mathbf{K}_{cj}^{-}(\mathbf{x}_c)\mathbf{1}_{l\times n}.
\end{aligned}$$

Form (20), (21), (22) and (23), the DET-PDOF controller gains are given as below:

$$\mathbf{K}_{cj}^{+}(\mathbf{x}_c) = \frac{\mathbf{1}_m\mathbf{O}_{cj}^{+}(\mathbf{x}_c)}{\left(\boldsymbol{\xi}_1{}^T + \boldsymbol{\xi}_2{}^T\right)\mathbf{B}_{\max}\mathbf{1}_m}, \quad (28)$$

$$\mathbf{K}_{cj}^{-}(\mathbf{x}_c) = \frac{\mathbf{1}_m\mathbf{O}_{cj}^{-}(\mathbf{x}_c)}{\left(\boldsymbol{\xi}_1{}^T + \boldsymbol{\xi}_2{}^T\right)\mathbf{B}_{\max}\mathbf{1}_m}, \quad (29)$$

$$\mathbf{a}_f^{cij}(\mathbf{x}_c) = \frac{\mathbf{m}_f^{cij}(\mathbf{x}_c)}{\boldsymbol{\xi}_2{}^T\mathbf{1}_n^{(f)}}, \quad (30)$$

$$\mathbf{b}_f^{cj}(\mathbf{x}_c) = \frac{\mathbf{n}_f^{cj}(\mathbf{x}_c)}{\boldsymbol{\xi}_2{}^T\mathbf{1}_n^{(f)}}. \quad (31)$$

Combining $\beta_1\big(\boldsymbol{\xi}_1{}^T + \boldsymbol{\xi}_2{}^T\big)\mathbf{B}_{\max}\mathbf{1}_m \leq \boldsymbol{\xi}_2{}^T\mathbf{1}_n^{(f)} \leq \beta_2\big(\boldsymbol{\xi}_1{}^T + \boldsymbol{\xi}_2{}^T\big)\mathbf{B}_{\max}\mathbf{1}_m$, it holds that

$$\begin{aligned}
&\tilde{\boldsymbol{\mathcal{A}}}_{ij}(\mathbf{x},\mathbf{x}_c) \geq \hat{\boldsymbol{\mathcal{A}}}_{ij}(\mathbf{x},\mathbf{x}_c), \\
&\tilde{\boldsymbol{\mathcal{A}}}_{ij}^{11}(\mathbf{x},\mathbf{x}_c) \geq \big(\boldsymbol{\xi}_1{}^T + \boldsymbol{\xi}_2{}^T\big)\mathbf{B}_{\max}\mathbf{1}_m\mathbf{A}_i(\mathbf{x}) \\
&\quad + \mathbf{B}_i(\mathbf{x})\sigma_2\big(\mathbf{I} + k_u\mathbf{1}_{m\times m}\big)\mathbf{1}_m\mathbf{O}_{cj}^{-}(\mathbf{x}_c)\mathbf{1}_{l\times n} \\
&\quad + \mathbf{B}_i(\mathbf{x})\big(\sigma_1\mathbf{I} - k_u\sigma_2\mathbf{1}_{m\times m}\big)\mathbf{1}_m\mathbf{O}_{cj}^{+}(\mathbf{x}_c)\mathbf{1}_{l\times n}, \quad (32) \\
&\tilde{\boldsymbol{\mathcal{A}}}_{ij}^{12}(\mathbf{x},\mathbf{x}_c) \geq -\mathbf{B}_i(\mathbf{x})\sigma_1\big(\mathbf{I} + k_u\mathbf{1}_{m\times m}\big)\mathbf{1}_m\mathbf{O}_{cj}^{-}(\mathbf{x}_c)\mathbf{1}_{l\times n} \\
&\quad - \mathbf{B}_i(\mathbf{x})\big(\sigma_2\mathbf{I} - k_u\sigma_1\mathbf{1}_{m\times m}\big)\mathbf{1}_m\mathbf{O}_{cj}^{+}(\mathbf{x}_c)\mathbf{1}_{l\times n}, \quad (33) \\
&\tilde{\boldsymbol{\mathcal{A}}}_{ij}^{21}(\mathbf{x},\mathbf{x}_c) \geq \boldsymbol{\xi}_2{}^T\mathbf{1}_n^{(f)}\mathbf{A}_i(\mathbf{x}) - \mathbf{n}_f^{cj}(\mathbf{x}_c)\left(\mathbf{I} + k_y\mathbf{1}_{l\times l}\right)\mathbf{C}_i(\mathbf{x}) \\
&\quad - \mathbf{m}_f^{cij}(\mathbf{x}_c) + \mathbf{B}_i(\mathbf{x})\big(\beta_1\sigma_1\mathbf{I} - \beta_2k_u\sigma_2\mathbf{1}_{m\times m}\big)\mathbf{1}_m\mathbf{O}_{cj}^{+}(\mathbf{x}_c)\mathbf{1}_{l\times n} \\
&\quad + \beta_2\mathbf{B}_i(\mathbf{x})\sigma_2\big(\mathbf{I} + k_u\mathbf{1}_{m\times m}\big)\mathbf{1}_m\mathbf{O}_{cj}^{-}(\mathbf{x}_c)\mathbf{1}_{l\times n}, \quad (34) \\
&\tilde{\boldsymbol{\mathcal{A}}}_{ij}^{22}(\mathbf{x},\mathbf{x}_c) \geq -\mathbf{B}_i(\mathbf{x})\big(\beta_2\sigma_2\mathbf{I} - \beta_1k_u\sigma_1\mathbf{1}_{m\times m}\big)\mathbf{1}_m\mathbf{O}_{cj}^{+}(\mathbf{x}_c)\mathbf{1}_{l\times n} \\
&\quad - \beta_1\mathbf{B}_i(\mathbf{x})\sigma_1\big(\mathbf{I} + k_u\mathbf{1}_{m\times m}\big)\mathbf{1}_m\mathbf{O}_{cj}^{-}(\mathbf{x},\mathbf{x}_c)\mathbf{1}_{l\times n} + \mathbf{m}_f^{cij}(\mathbf{x}_c). \quad (35)
\end{aligned}$$

Therefore, the augmented system (13) is proved to be positive if conditions $\tilde{\boldsymbol{\mathcal{A}}}_{ij}(\mathbf{x},\mathbf{x}_c)$ are Metzler, $\boldsymbol{\mathcal{B}}_{wij}(\mathbf{x}) \geq 0, \boldsymbol{\mathcal{D}}_{ij}(\mathbf{x},\mathbf{x}_c) \geq 0, \boldsymbol{\mathcal{E}}_{wi}(\mathbf{x}) \geq 0$ are fulfilled. The SOS-based positivity sufficiency conditions for the augmented system (13) can be derived in follow Theorem.

*Theorem 2:* For given positive scalars $\varepsilon$, $\gamma$, $0 < k \leq 1$, $0 < k_c \leq 1$, $0 \leq \beta_1 \leq \beta_2$, $0 \leq \sigma_1 \leq \sigma_2$, vectors $\boldsymbol{\xi}_1, \boldsymbol{\xi}_2 \succ 0$, the dual-event-based PPFS (13) is positive such that

$$\begin{aligned}
&\tilde{\boldsymbol{\mathcal{A}}}_{ij}^{11,(f,s)}(\mathbf{x},\mathbf{x}_c) - \nu(\mathbf{x},\mathbf{x}_c) \text{ is SOS}, i \in \underline{n_p}, j \in \underline{n_c}, f \neq s \in \underline{n} \\
&\tilde{\boldsymbol{\mathcal{A}}}_{ij}^{12,(f,s)}(\mathbf{x},\mathbf{x}_c) - \nu(\mathbf{x},\mathbf{x}_c) \text{ is SOS}, i \in \underline{n_p}, j \in \underline{n_c}, f = s \in \underline{n} \\
&\tilde{\boldsymbol{\mathcal{A}}}_{ij}^{21,(f,s)}(\mathbf{x},\mathbf{x}_c) - \nu(\mathbf{x},\mathbf{x}_c) \text{ is SOS}, i \in \underline{n_p}, j \in \underline{n_c}, f = s \in \underline{n} \\
&\tilde{\boldsymbol{\mathcal{A}}}_{ij}^{22,(f,s)}(\mathbf{x},\mathbf{x}_c) - \nu(\mathbf{x},\mathbf{x}_c) \text{ is SOS}, i \in \underline{n_p}, j \in \underline{n_c}, f \neq s \in \underline{n} \\
&\boldsymbol{\xi}_2{}^T\mathbf{1}_n^{(f)} - \beta_1\big(\boldsymbol{\xi}_1{}^T + \boldsymbol{\xi}_2{}^T\big)\mathbf{B}_{\max}\mathbf{1}_m - \nu(\mathbf{x}) \text{ is SOS}, f \in \underline{n} \\
&\beta_2\big(\boldsymbol{\xi}_1{}^T + \boldsymbol{\xi}_2{}^T\big)\mathbf{B}_{\max}\mathbf{1}_m - \boldsymbol{\xi}_2{}^T\mathbf{1}_n^{(f)} - \nu(\mathbf{x}) \text{ is SOS}, f \in \underline{n} \\
&\sigma_2 - \mathbf{C}_c^{(f,s)} - \nu \text{ is SOS}, j \in \underline{n_c}, f \in \underline{l}, s \in \underline{n} \\
&\mathbf{C}_c^{(f,s)} - \sigma_1 - \nu \text{ is SOS}, j \in \underline{n_c}, f \in \underline{l}, s \in \underline{n} \\
&\mathbf{C}_i^{(f,s)}(\mathbf{x}) - \nu(\mathbf{x}) \text{ is SOS}, i \in \underline{n_p}, f \in \underline{l}, s \in \underline{n} \\
&\mathbf{B}_{wi}^{(f,s)}(\mathbf{x}) - \nu(\mathbf{x}) \text{ is SOS}, i \in \underline{n_p}, f \in \underline{n}, s \in \underline{r} \\
&\mathbf{E}_{wi}^{(f,s)}(\mathbf{x}) - \nu(\mathbf{x}) \text{ is SOS}, i \in \underline{n_p}, f \in \underline{q}, s \in \underline{r}
\end{aligned}$$

where $\nu > 0$ is predefined scalar. $\mathbf{C}_c = \left(c_{fs}^c\right) \in \Re^{l\times n}$, $\mathbf{C}_c^{(f,s)} = c_{fs}^c$, $\mathbf{B}_{wi}(\mathbf{x}) = \left(b_{fs}^{wi}(\mathbf{x})\right) \in \Re^{n\times r}$, $\mathbf{B}_{wi}^{(f,s)}(\mathbf{x}) = b_{fs}^{wi}(\mathbf{x})$ and $\mathbf{E}_{wi}(\mathbf{x}) = \left(e_{fs}^{wi}\right) \in \Re^{q\times r}$, $\mathbf{E}_{wi}^{(f,s)}(\mathbf{x}) = e_{fs}^{wi}(\mathbf{x})$. $\tilde{\boldsymbol{\mathcal{A}}}_{ij}^{mn,(f,s)}(\mathbf{x},\mathbf{x}_c)$, $m,n \in \{1,2\}$ are defined in (32), (33), (34) and (35). The PDOF controller gains are defined in (28), (29), (30) and (31).

*Remark 5:* Due to the introduction of new state variables, the order of the dual-event-based augmented systems (13) increases, and the nonconvex conditions become more complex. To handle the nonconvex terms introduced by the coupled PDOF gains $\mathbf{A}_{cij}(\mathbf{x}_c)$, $\mathbf{B}_{cj}(\mathbf{x}_c)$, $\mathbf{C}_c$ and $\mathbf{K}_{cj}(\mathbf{x}_c)$, we design a novel convexification strategy by establishing specific bounds on $\mathbf{C}_c$ and constructing auxiliary variables (20)-(23) to replace the nonconvex terms in the stability conditions. In the positivity analysis, the inconsistent denominators among the control gains in (28)-(31) are resolved by imposing a bounding constraint $\beta_1\big(\boldsymbol{\xi}_1{}^T + \boldsymbol{\xi}_2{}^T\big)\mathbf{B}_{\max}\mathbf{1}_m \leq \boldsymbol{\xi}_2{}^T\mathbf{1}_n^{(f)} \leq \beta_2\big(\boldsymbol{\xi}_1{}^T + \boldsymbol{\xi}_2{}^T\big)\mathbf{B}_{\max}\mathbf{1}_m$. This critical step successfully transforms the intractable nonconvex positivity constraints into convex SOS-based conditions, thereby ensuring the solvability of the proposed scheme via SOSTOOLS.

*Remark 6:* A positive system is defined by the non-negativity of its closed-loop state response, rather than by non-negative control inputs. Even if the input is negative, the system can still maintain positivity provided that the system matrix $A_i(x)$ is Metzler and the input matrix satisfies

$B_i(x) \geq 0$.

## IV. IT2 MFD Control for IT2 Dual-event-based Augmented Closed-Loop System

### A. Multivariable Chebyshev Embedded Type-1 Membership Functions Based on IGA

Inspired by [38], multivariable Chebyshev MFs with minimum approximation error are used as the polynomial function with the best approximation degree to deal with the embedded type-1 MFs $\tilde{h}_{ij}(\mathbf{x}, \hat{\mathbf{y}}_c) = \tilde{w}_i(\mathbf{x})\,\tilde{m}_j(\hat{\mathbf{y}}_c)$. It takes the following form

$$\begin{aligned}\hat{h}^*_{ij}\left(\zeta^*_{ij}\middle|\,\mathbf{x},\mathbf{x}_c\right) &= \sum\nolimits_{g=1}^{s} a^*_{ijg}\varsigma_g(\mathbf{x},\mathbf{x}_c) \\ &= \tilde{h}_{ij}(\mathbf{x},\hat{\mathbf{y}}_c) - \left\|\Delta h^*_{iji}\left(\zeta^*_{ij}\middle|\,\mathbf{x},\mathbf{x}_c\right)\right\|_\infty, \quad (36)\end{aligned}$$

$$\begin{aligned}&\left\|\Delta h^*_{iji}\left(\zeta^*_{ij}\middle|\,\mathbf{x},\mathbf{x}_c\right)\right\|_\infty \\ &= \inf_{\hat{h}_{ij}\left(\zeta^*_{ij}\middle|\mathbf{x},\mathbf{x}_c\right)\in\mathcal{H}} \max_{\mathbf{x},\hat{\mathbf{y}}_c\in\mathcal{X}} \left|\tilde{h}_{ij}(\mathbf{x},\hat{\mathbf{y}}_c) - \hat{h}_{ij}\left(\zeta_{ij}\middle|\,\mathbf{x},\mathbf{x}_c\right)\right|, \quad (37)\end{aligned}$$

where $\mathcal{H} = span\{\varsigma_s(\mathbf{x},\mathbf{x}_c), \varsigma_{s-1}(\mathbf{x},\mathbf{x}_c), ..., \varsigma_1(\mathbf{x},\mathbf{x}_c), 1\}$, $\mathcal{X}$ is a predefined compact subset of Banach space.

However, how to obtain more accurate multivariable Chebyshev MFs by optimizing the Chebyshev error is the critical issue. The process of multivariable Chebyshev MFs optimization is represented by the following Algorithm.

$$\begin{aligned}\mathbf{P}: \quad &\textbf{min} \quad \max_{\mathbf{x},\mathbf{x}_c\in\mathcal{X}} \left|\tilde{h}_{ij}(\mathbf{x},\hat{\mathbf{y}}_c) - \hat{h}_{ij}\left(\zeta_{ij}\middle|\,\mathbf{x},\mathbf{x}_c\right)\right| \\ &\textbf{subject to} \quad \mathcal{X} = \{(x_1,...,x_n)| -\infty \prec x_s \prec \infty, s\in[1,n]\}.\end{aligned}$$

*Remark 7:* As shown in (36) and (37), the Chebyshev MFs $\hat{h}^*_{ij}\left(\zeta^*_{ij}\middle|\,\mathbf{x},\mathbf{x}_c\right)$ constitute the optimal solution in a given finite dimensional linear subspace $\mathcal{H}$ [38]. Note that the solution to the optimization problem **P** (finding the minimal multivariate polynomial error) involves a multi-dimensional space spanned by the state $\mathbf{x}$ and $\mathbf{x}_c$. Therefore, we propose an IGA to solve this multidimensional function extremum problem, which is suitable for the optimization process of problem **P**, and can quickly find more accurate multivariate Chebyshev MFs.

*Remark 8:* The innovation of IGA is embodied in two aspects. One is Step 9 of the IGA, which selects the $n = mp{\cdot}P$ elite individuals to be retained before the selection operation, so as to avoid the elite individuals being accidentally eliminated in the subsequent operation. The second is Step 11 of the algorithm, in the crossover operation, the population after the crossover and the population before the crossover are combined. The combined population is sorted by the Chebyshev error and the optimal individuals are selected to form a new population, which will provide an excellent population base for the subsequent operations.

**Algorithm:** Multivariable Chebyshev MFs Optimization Based on IGA

1: Initialize the number of population, chromosome lchrom and maximum generation as: $P \leftarrow$ popsize, $I \leftarrow$ lchrom and $G \leftarrow$ generation
2: OLDPOP $\leftarrow$ generateRandomPopulation ($P$, $I$)
3: **for** gen=1:maxgen
4: $a^s_{ij} \in \left[al^s_{ij}, au^s_{ij}\right] \leftarrow$ applyTaylor ($\tilde{h}_{ij}$)
5: **for** $i = 1 : P$
6: Calculates the state quantity in the interval that maximizes the error $|\Delta h_{ij}(\zeta_{ij}|\,\mathbf{x},\mathbf{x}_c)|$ as: $\left[\mathbf{x}^i_m, \mathbf{x}^i_{cm}\right] \leftarrow$ solveMax ($a^s_{ij}$)
7: The maximum error is defined as: $\text{Fit}(i) = \left|\tilde{h}_{ij}\left(\mathbf{x}^i_m,\mathbf{x}^i_{cm}\right) - \hat{h}_{ij}\left(\zeta_{ij}\middle|\,\mathbf{x}^i_m,\mathbf{x}^i_{cm}\right)\right|$
8: Rank the Fitness from largest to smallest and find the MaxFitness and its $a^s_{ij}$
9: EPOP $\leftarrow$ retainEliteIndividuals (OLDPOP, $mp{\cdot}P$)
10: TEMP $\leftarrow$ applySelect (OLDPOP)
11: **if** $rand < pcross$ **then** cTEMP $\leftarrow$ applyCrossover (TEMP, $Pcross$) **end**
12: **if** $rand < Pmuta$ **then** OLDPOP $\leftarrow$ applyMutation (cTEMP, $Pmuta$) **end**
13: OLDPOP $\leftarrow$ retainEliteIndividuals (EPOP, $mp{\cdot}P$)
14: **end**
15: **end**
16: (BestGEN, BestFIT)$\leftarrow$ getBest (OLDPOP)
17: **Output**: $\left\|\Delta h^*_{iji}\left(\zeta^*_{iji}\middle|\,\mathbf{x},\mathbf{x}_c\right)\right\|_\infty$, $a^*_{ij}$ and $G_{best}$

### B. Multivariable IT2-MFD Analysis for Dual-event-based Augmented Closed-Loop System

Now, the relaxed IT2 stability conditions can be obtained by introducing multivariable embedded type-1 MFs and chebyshev error calculated by the IGA. Define slack matrices $0 < \mathbf{Y}_{iji}(\mathbf{x},\mathbf{x}_c) \in \Re^{1\times n}$, satisfy $\sum_{\iota=1}^{\varepsilon}\vartheta_\iota\mathbf{Y}_{iji}(\mathbf{x},\mathbf{x}_c) - \tilde{\mathbf{\Xi}}_{ij}(\mathbf{x},\mathbf{x}_c) \geq 0$. Combining (36) and (37),

$$\begin{aligned}\dot{\mathbf{V}}(\mathbf{x},\mathbf{x}_c) &\leq \sum_{i=1}^{n_p}\sum_{j=1}^{n_c}\tilde{h}_{ij}(\mathbf{x},\hat{\mathbf{y}}_c)\tilde{\mathbf{\Xi}}_{ij}(\mathbf{x},\mathbf{x}_c)\boldsymbol{\chi} \\ &\leq \sum_{i=1}^{n_p}\sum_{j=1}^{n_c}\Big(\hat{h}^*_{ij}\left(\zeta^*_{iji}\middle|\,\mathbf{x},\mathbf{x}_c\right)\tilde{\mathbf{\Xi}}_{ij}(\mathbf{x},\mathbf{x}_c) + \sum_{\iota=1}^{\varepsilon}\vartheta_\iota \\ &\quad\times\left\|\Delta h^*_{iji}\left(\zeta^*_{iji}\middle|\,\mathbf{x},\mathbf{x}_c\right)\right\|_\infty\mathbf{Y}_{iji}(\mathbf{x},\mathbf{x}_c)\Big)\boldsymbol{\chi}. \quad (38)\end{aligned}$$

In addition, by introducing the boundary information of the operating domain, we restrict the stability conditions to the local subspaces defined by $x_g \in [x_{g1}, x_{g2}]$ and $x^c_g \in \left[x^c_{g1}, x^c_{g2}\right]$, $g = 1, 2, ..., n$, thereby reducing the conservatism of the stability analysis. For this reason, we have the following constraints:

$$\begin{aligned}&\sum_{\iota=1}^{\varepsilon}\vartheta_\iota\Big(\sum_{g=1}^{n}(x_g - x_{g1\iota})(x_{g2\iota} - x_g) \\ &\quad+\sum_{g=1}^{n}\left(x^c_g - x^c_{g1\iota}\right)\left(x^c_{g2\iota} - x^c_g\right)\Big)\mathbf{N}_{g\iota}(\mathbf{x},\mathbf{x}_c) \geq 0. \quad (39)\end{aligned}$$

where define slack matrices $\mathbf{N}_{g\iota}(\mathbf{x},\mathbf{x}_c) \in \Re^{1\times n}$, satisfy $\mathbf{N}_{g\iota}(\mathbf{x},\mathbf{x}_c) \geq 0$. From (39),

$$\dot{\mathbf{V}}(\mathbf{x},\mathbf{x}_c) \leq \sum_{\iota=1}^{\varepsilon} \vartheta_\iota \sum_{i=1}^{n_p}\sum_{j=1}^{n_c} \Big( \hat{h}_{ij}^* \left(\zeta_{ij\iota}^* \middle| \mathbf{x},\mathbf{x}_c\right) \tilde{\mathbf{\Xi}}_{ij}(\mathbf{x},\mathbf{x}_c) + \left\|\Delta h_{ij\iota}^* \left(\zeta_{ij\iota}^* \middle| \mathbf{x},\mathbf{x}_c\right)\right\|_\infty \mathbf{Y}_{ij\iota}(\mathbf{x},\mathbf{x}_c) + \Big( \sum_{g=1}^{n} (x_g - x_{g1\iota}) \times (x_{g2\iota} - x_g) + \sum_{g=1}^{n} \big(x_g^c - x_{g1\iota}^c\big)\big(x_{g2\iota}^c - x_g^c\big)\Big)\mathbf{N}_{g\iota}(\mathbf{x},\mathbf{x}_c)\Big)\boldsymbol{\chi}. \quad (40)$$

Besides, define slack matrices $0 < \mathbf{Z}_{i\iota}(\mathbf{x},\mathbf{x}_c) \in \Re^{1\times n}$, satisfy $\sum_{\iota=1}^{\varepsilon} \vartheta_\iota \mathbf{Z}_{i\iota}(\mathbf{x},\mathbf{x}_c) - \mathbf{\Psi}_i(\mathbf{x},\mathbf{x}_c) \geq 0$. Combining (26), (36) and (37),

$$\mathbf{J}(\mathbf{x},\mathbf{x}_c) \leq \sum_{\iota=1}^{\varepsilon} \vartheta_\iota \sum_{i=1}^{n_p}\sum_{j=1}^{n_c} \Big( \hat{h}_{ij}^* \left(\zeta_{ij\iota}^* \middle| \mathbf{x},\mathbf{x}_c\right) \mathbf{\Psi}_i(\mathbf{x}) + \left\|\Delta h_{ij\iota}^* \left(\zeta_{ij\iota}^* \middle| \mathbf{x},\mathbf{x}_c\right)\right\|_\infty \mathbf{Z}_{i\iota}(\mathbf{x},\mathbf{x}_c) + \Big( \sum_{g=1}^{n} (x_g - x_{g1\iota})(x_{g2\iota} - x_g) + \sum_{g=1}^{n} \big(x_g^c - x_{g1\iota}^c\big)\big(x_{g2\iota}^c - x_g^c\big)\Big)\mathbf{N}_{g\iota}(\mathbf{x},\mathbf{x}_c)\Big)\mathbf{w} - \mathbf{V}(\mathbf{x},\mathbf{x}_c). \quad (41)$$

*Remark 9:* Since Theorem 1 ignores the IT2-MFs, the stability conditions are conservative. From (38), the IT2-MFs $\tilde{h}_{ij}(\mathbf{x},\hat{\mathbf{y}}_c) = \tilde{w}_i(\mathbf{x})\,\tilde{m}_j(\hat{\mathbf{y}}_c)$ are transformed into approximating embedded type-1 MFs and their bounded approximation errors, leading to the relaxation of the stability conditions. Consequently, this relaxation allows for a wider feasible range of event-triggered threshold selection, enhancing the design flexibility.

*Remark 10:* A major challenge arises from the mismatched premise variables, where $\tilde{w}_i(\mathbf{x})$ depend on $\mathbf{x}$ and $\tilde{m}_j(\hat{\mathbf{y}}_c)$ depend on $\hat{\mathbf{y}}_c$, complicating the MFD analysis. We combine the DET mechanism (10) and output dynamics to address the issue of asynchronous premise variables in the PDOF control process. The method is divided into the following two steps: *Step 1. Estimate* $\mathbf{y}_c\left(t_q^u\right)$ *by* $\mathbf{y}_c(t)$: According to the event-triggered condition (10), (12) couples $\mathbf{y}_c(t_q^u)$ and $\mathbf{y}_c(t)$, and depends on the polynomial matrices $\mathbf{K}_{cj}(\mathbf{x}_c)$. We introduce a linear constraint on the possible range of values for $\mathbf{y}_c(t_q^u)$, which can be defined as

$$\left|\mathbf{y}_c(t_q^u) - \mathbf{y}_c(t)\right| \leq \omega_{\max} \left|\mathbf{y}_c(t)\right| + \rho_{\max}\mathbf{1}_l, \quad (42)$$

where $\omega_{\max}$ and $\rho_{\max}$ are positive constants.

*Step 2. Output dynamics*: Combining $\sigma_1\mathbf{1}_{l\times n} \leq \mathbf{C}_c \leq \sigma_2\mathbf{1}_{l\times n}$, (42) can be rewritten as

$$\begin{aligned}\mathbf{C}_c\mathbf{x}_c(t) - \omega_{\max}\mathbf{C}_c\mathbf{x}_c(t) - \rho_{\max}\mathbf{1}_l &\leq \mathbf{y}_c(t_q^u) \\ &\leq \mathbf{C}_c x_c(t) + \omega_{\max}\mathbf{C}_c\mathbf{x}_c(t) + \rho_{\max}\mathbf{1}_l. \quad (43)\end{aligned}$$

Then, the relationship between the asynchronous premise variables is as follows:

$$\begin{aligned}(\sigma_1 - \omega_{\max}\sigma_2)\,\mathbf{1}_{l\times n}\mathbf{x}_c(t) - \rho_{\max}\mathbf{1}_l &\leq \mathbf{y}_c(t_q^u) \\ &\leq (1+\omega_{\max})\sigma_2\mathbf{1}_{l\times n}\mathbf{x}_c(t) + \rho_{\max}\mathbf{1}_l. \quad (44)\end{aligned}$$

Next, the SOS-based conditions are derived as follows.

*Theorem 3:* For given positive scalars $\varepsilon$, $\gamma$, $0 < k \leq 1$, $0 < k_c \leq 1$, $0 \leq \alpha_1 \leq 1$, $0 \leq \alpha_2 \leq 1$, vectors $\boldsymbol{\xi}_1, \boldsymbol{\xi}_2 \succ 0$, the dual-event-based PPFS (13) is asymptotically stable with $L_1$-gain performance such that

$$-\Bigg(\sum_{\iota=1}^{\varepsilon} \vartheta_\iota \sum_{i=1}^{n_p}\sum_{j=1}^{n_c} \Big( \hat{h}_{ij\iota}^* \left(\zeta_{ij\iota}^* \middle| \mathbf{x},\mathbf{x}_c\right) \tilde{\Xi}_{ij\iota}^f(\mathbf{x},\mathbf{x}_c) + \left\|\Delta h_{ij\iota}^* \left(\zeta_{ij\iota}^* \middle| \mathbf{x},\mathbf{x}_c\right)\right\|_\infty Y_{ij\iota}^f(\mathbf{x},\mathbf{x}_c) + \Big( \sum_{g=1}^{n} (x_g - x_{g1\iota}) \times (x_{g2\iota} - x_g) + \sum_{g=1}^{n} \big(x_g^c - x_{g1\iota}^c\big)\big(x_{g2\iota}^c - x_g^c\big)\Big)N_{g\iota}^f(\mathbf{x},\mathbf{x}_c)\Big) + \nu(\mathbf{x},\mathbf{x}_c)\Bigg) \text{ is SOS}, i \in \underline{n_p}, j \in \underline{n_c}, f \in \underline{n} \quad (45)$$

$$-\Bigg(\sum_{\iota=1}^{\varepsilon} \vartheta_\iota \sum_{i=1}^{n_p}\sum_{j=1}^{n_c} \Big( \hat{h}_{ij\iota}^* \left(\zeta_{ij\iota}^* \middle| \mathbf{x},\mathbf{x}_c\right) \Psi_{i\iota}^f(\mathbf{x}) + \left\|\Delta h_{ij\iota}^* \left(\zeta_{ij\iota}^* \middle| \mathbf{x},\mathbf{x}_c\right)\right\|_\infty Z_{i\iota}^f(\mathbf{x},\mathbf{x}_c) + \Big( \sum_{g=1}^{n} (x_g - x_{g1\iota}) \times (x_{g2\iota} - x_g) + \sum_{g=1}^{n} \big(x_g^c - x_{g1\iota}^c\big)\big(x_{g2\iota}^c - x_g^c\big)\Big)N_{g\iota}^f(\mathbf{x},\mathbf{x}_c)\Big) + \nu(\mathbf{x},\mathbf{x}_c)\Bigg) \text{ is SOS}, i \in \underline{n_p}, j \in \underline{n_c}, f \in \underline{n} \quad (46)$$

$$Y_{ij\iota}^f(\mathbf{x},\mathbf{x}_c) - \tilde{\Xi}_{ij\iota}^f(\mathbf{x},\mathbf{x}_c) \text{ is SOS}, i \in \underline{n_p}, j \in \underline{n_c}, f \in \underline{n} \quad (47)$$

$$Z_{i\iota}^f(\mathbf{x},\mathbf{x}_c) - \Psi_{i\iota}^f(\mathbf{x}) \text{ is SOS}, i \in \underline{n_p}, j \in \underline{n_c}, f \in \underline{n} \quad (48)$$

$$Y_{ij\iota}^f(\mathbf{x},\mathbf{x}_c) \text{ is SOS}, i \in \underline{n_p}, j \in \underline{n_c}, f \in \underline{n} \quad (49)$$

$$Z_{i\iota}^f(\mathbf{x},\mathbf{x}_c) \text{ is SOS}, i \in \underline{n_p}, f \in \underline{n} \quad (50)$$

$$N_{g\iota}^f(\mathbf{x},\mathbf{x}_c) \text{ is SOS}, i \in \underline{n_p}, j \in \underline{n_c}, f \in \underline{n} \quad (51)$$

where $\tilde{\Xi}_{ij\iota}^f(\mathbf{x},\mathbf{x}_c)$, $\Psi_{i\iota}^f(\mathbf{x})$, $Y_{ij\iota}^f(\mathbf{x},\mathbf{x}_c)$, $Z_{i\iota}^f(\mathbf{x},\mathbf{x}_c)$ and $N_{g\iota}^f(\mathbf{x},\mathbf{x}_c)$ are the $f^{th}$ element of vector $\tilde{\mathbf{\Xi}}_{ij\iota}(\mathbf{x},\mathbf{x}_c)$, $\mathbf{\Psi}_{i\iota}(\mathbf{x})$, $\mathbf{Y}_{ij\iota}(\mathbf{x},\mathbf{x}_c)$, $\mathbf{Z}_{ij\iota}(\mathbf{x},\mathbf{x}_c)$ and $\mathbf{N}_{g\iota}(\mathbf{x},\mathbf{x}_c)$.

### C. Analysis of Zeno Behavior

The following proof is used to exclude the Zeno behavior in the DET mechanisms (9) and (10).

*Part I:* The derivative of error $\mathbf{e}_y(t)$ on $\left[t_p^y, t_{p+1}^y\right)$ is

$$D^+\mathbf{e}_y(t) = -\sum_{i=1}^{n_p}\sum_{j=1}^{n_c} \tilde{h}_{ij}(\mathbf{x},\hat{\mathbf{y}}_c) \sum_{s=1}^{n_p} \tilde{w}_s(\mathbf{x})\,\mathbf{C}_s(\mathbf{x})\Big(\mathbf{A}_i(\mathbf{x}) \times \mathbf{x}(t) + \mathbf{B}_i(\mathbf{x})\mathbf{K}_{cj}(\mathbf{x}_c)\mathbf{C}_c\mathbf{x}_c\left(t_q^u\right) + \mathbf{B}_{wi}(\mathbf{x})\mathbf{w}(t)\Big), \quad (52)$$

Then, one obtains

$$\begin{aligned}D^+\left\|\mathbf{e}_y(t)\right\| \leq \sum_{i=1}^{n_p}\sum_{j=1}^{n_c} \tilde{h}_{ij}(\mathbf{x},\hat{\mathbf{y}}_c)\Bigg( &\left\|\mathbf{A}_i(\mathbf{x})\right\| \left\|\mathbf{e}_y(t)\right\| \\ &+ \left\|\sum_{s=1}^{n_p} \tilde{w}_s(\mathbf{x})\mathbf{C}_s(\mathbf{x})\mathbf{A}_i(\mathbf{x})\right\| \left\|\mathbf{x}\left(t_p^y\right)\right\| \\ &+ \left\|\sum_{s=1}^{n_p} \tilde{w}_s(\mathbf{x})\mathbf{C}_s(\mathbf{x})\mathbf{B}_i(\mathbf{x})\mathbf{K}_{cj}(\mathbf{x}_c)\mathbf{C}_c\right\| \left\|\mathbf{x}_c\left(t_q^u\right)\right\|\end{aligned}$$

$$+\left\|\sum_{s=1}^{n_p}\tilde{w}_s\left(\mathbf{x}\right)\mathbf{C}_s(\mathbf{x})\mathbf{B}_{wi}(\mathbf{x})\right\|\left\|\mathbf{w}\left(t\right)\right\|\Big), \tag{53}$$

which means that $D^+\left\|\mathbf{e}_y\left(t\right)\right\| \le a_1\left\|\mathbf{e}_y\left(t\right)\right\| + a_2$ with $a_1 = \sum_{i=1}^{n_p}\sum_{j=1}^{n_c}\tilde{h}_{ij}\left(\mathbf{x},\hat{\mathbf{y}}_c\right)\|\mathbf{A}_i(\mathbf{x})\|$ and $a_2$ is the upper bound of $\sum_{i=1}^{n_p}\sum_{j=1}^{n_c}\tilde{h}_{ij}\left(\mathbf{x},\hat{\mathbf{y}}_c\right)\left(\left\|\sum_{s=1}^{n_p}\tilde{w}_s\left(\mathbf{x}\right)\mathbf{C}_s(\mathbf{x})\mathbf{A}_i(\mathbf{x})\right\|\left\|\mathbf{x}\left(t_p^y\right)\right\| + \left\|\sum_{s=1}^{n_p}\tilde{w}_s\left(\mathbf{x}\right)\mathbf{C}_s(\mathbf{x})\mathbf{B}_i(\mathbf{x})\mathbf{K}_{cj}(\mathbf{x}_c)\mathbf{C}_c\right\|\left\|\mathbf{x}_c\left(t_q^u\right)\right\| + \left\|\sum_{s=1}^{n_p}\tilde{w}_s\left(\mathbf{x}\right)\ \mathbf{C}_s(\mathbf{x})\mathbf{B}_{wi}(\mathbf{x})\right\|\left\|\mathbf{w}\left(t\right)\right\|\right)$. We denote $\mathbf{w}\left(t\right)$ that is essentially bounded and belongs to $L_1\left[0,\infty\right)$ with its $L_1$-norm $\left\|\mathbf{w}\left(t\right)\right\|_{L_1} = \int_{t=0}^{\infty}\left\|w\left(t\right)\right\|_1 < \infty$. The boundedness of $\mathbf{x}\left(t\right)$ and $\mathbf{x}_c\left(t\right)$ can be ensured in the stability analysis of the paper. Then, by integrating both sides of $D^+\left\|\mathbf{e}_y\left(t\right)\right\| \le a_1\left\|\mathbf{e}_y\left(t\right)\right\| + a_2$ from $t_p^y$ to $t$, we can obtain

$$\left\|\mathbf{e}_y\left(t\right)\right\| \le \frac{a_2}{a_1}\left(\mathbf{e}^{a_1\left(t-t_p^y\right)}-1\right), \tag{54}$$

from event-triggered condition (9), the next data transmission instant $t_{p+1}^y$ satisfies

$$k_y\Big(\left\|\hat{\mathbf{y}}\left(t_p^y\right)\right\|_1 - \left\|\mathbf{e}_y\left(t_{p+1}^y\right)\right\|_1\Big) \le \left\|\mathbf{e}_y\left(t_{p+1}^y\right)\right\|_1. \tag{55}$$

Moreover, based on the relationship between the 1-norm and 2-norm, it further indicates

$$\left\|\mathbf{e}_y\left(t_{p+1}^y\right)\right\|_1 \le \sqrt{n}\left\|\mathbf{e}_y\left(t_{p+1}^y\right)\right\|, \tag{56}$$

Then, combining with (54), (55) and (56), we obtain

$$\frac{k_y\left\|\hat{\mathbf{y}}\left(t_p^y\right)\right\|_1}{\sqrt{n}\left(1+k_y\right)} \le \left\|\mathbf{e}_y\left(t_{p+1}^y\right)\right\| \le \frac{a_2}{a_1}\left(\mathbf{e}^{a_1\left(t_{p+1}^y-t_p^y\right)}-1\right), \tag{57}$$

finally, noting $\mathbf{e}_y\left(t_p^y\right)=0$, the triggered interval is

$$t_{p+1}^y - t_p^y \ge \frac{1}{a_1}\ln\left(1+\frac{a_1k_y\left\|\hat{\mathbf{y}}\left(t_p^y\right)\right\|_1}{a_2\sqrt{n}(1+k_y)}\right) \triangleq T_y^* > 0. \tag{58}$$

*Part II:* The derivative of error $\mathbf{e}_u\left(t\right)$ on $\left[t_q^u, t_{q+1}^u\right)$ is

$$D^+\left\|\mathbf{e}_u\left(t\right)\right\| \le \sum_{i=1}^{n_p}\sum_{j=1}^{n_c}\tilde{h}_{ij}\left(\mathbf{x},\hat{\mathbf{y}}_c\right)\Big(\left\|\mathbf{A}_{cij}(\mathbf{x}_c)\right\|\left\|\mathbf{e}_u\left(t\right)\right\| + \left\|\sum_{s=1}^{n_p}\sum_{f=1}^{n_c}\tilde{w}_s(\mathbf{x})\tilde{m}_f\left(\hat{\mathbf{y}}_c\right)\mathbf{K}_{cf}(\mathbf{x}_c)\mathbf{C}_c\mathbf{B}_{cj}(\mathbf{x}_c)\mathbf{C}_s(\mathbf{x})\right\|\left\|\mathbf{x}\left(t_p^y\right)\right\| + \left\|\sum_{f=1}^{n_c}\tilde{m}_f\left(\hat{\mathbf{y}}_c\right)\mathbf{K}_{cf}(\mathbf{x}_c)\mathbf{C}_c\mathbf{A}_{cij}(\mathbf{x}_c)\right\|\left\|\mathbf{x}_c\left(t_q^u\right)\right\|\Big), \tag{59}$$

which means that $D^+\left\|\mathbf{e}_u\left(t\right)\right\| \le b_1\left\|\mathbf{e}_u\left(t\right)\right\| + b_2$ with $b_1 = \sum_{i=1}^{n_p}\sum_{j=1}^{n_c}\tilde{h}_{ij}\left(\mathbf{x},\hat{\mathbf{y}}_c\right)\left\|\mathbf{A}_{cij}(\mathbf{x}_c)\right\|$ and $b_2$ is the upper bound of $\sum_{i=1}^{n_p}\sum_{j=1}^{n_c}\tilde{h}_{ij}\left(\mathbf{x},\hat{\mathbf{y}}_c\right)\Big(\left\|\sum_{f=1}^{n_c}\tilde{m}_f\left(\hat{\mathbf{y}}_c\right)\mathbf{K}_{cf}(\mathbf{x}_c)\mathbf{C}_c\mathbf{A}_{cij}(\mathbf{x}_c)\right\|\left\|\mathbf{x}_c\left(t_q^u\right)\right\| + \left\|\sum_{s=1}^{n_p}\times\sum_{f=1}^{n_c}\tilde{w}_s(\mathbf{x})\tilde{m}_f\left(\hat{\mathbf{y}}_c\right)\mathbf{K}_{cf}(\mathbf{x}_c)\mathbf{C}_c\mathbf{B}_{cj}(\mathbf{x}_c)\mathbf{C}_s(\mathbf{x})\right\|\left\|\mathbf{x}\left(t_p^y\right)\right\|\Big)$. Then, it follows that at $t\in\left[t_q^u, t_{q+1}^u\right)$,

$$\left\|\mathbf{e}_u\left(t\right)\right\| \le \frac{b_2}{b_1}\left(\mathbf{e}^{b_1\left(t-t_q^u\right)}-1\right), \tag{60}$$

from event-triggered condition (10), the next data transmission instant $t_{q+1}^u$ satisfies

$$\frac{k_u(\left\|\hat{\mathbf{u}}\left(t_q^u\right)\right\|_1 - \left\|\mathbf{e}_u\left(t_{q+1}^u\right)\right\|_1)}{\sqrt{n}} \le \frac{\left\|\mathbf{e}_u\left(t_{q+1}^u\right)\right\|_1}{\sqrt{n}} \le \left\|\mathbf{e}_u\left(t_{q+1}^u\right)\right\|, \tag{61}$$

finally, noting $\mathbf{e}_u\left(t_q^u\right)=0$, the triggered interval is

$$t_{q+1}^u - t_q^u \ge \frac{1}{b_1}\ln\left(1+\frac{b_1k_u\left\|\hat{\mathbf{u}}\left(t_q^u\right)\right\|_1}{b_2\sqrt{n}(1+k_u)}\right) \triangleq T_u^* > 0. \tag{62}$$

Consequently, for the DET schemes (9) and (10) in the S-C and C-A channels, the Zeno behavior is excluded.

*Theorem 4:* For any data transmission instants $\{t_p^y\}$ and $\{t_q^u\}$, there exist two positive constants $T_y^*$ and $T_u^*$ such that $t_{p+1}^y - t_p^y \ge T_y^*$, $t_{q+1}^u - t_q^u \ge T_u^*$, then the Zeno behavior is eliminated in the designed DET schemes (9) and (10).

## V. Illustrative Examples

**Example 1.** The matrices of the PPFSs with a 3-rule PFM are presented as follows for the $\mathbf{x}(t) = [x_1(t)\ x_2(t)]^T$ and $\mathbf{x}_c(t) = [x_{c1}(t)\ x_{c2}(t)]^T$.

$$\mathbf{A}_1(\mathbf{x})=\begin{bmatrix}-0.6-0.01x_1 & 0.50\\ 0.50 & -0.40\end{bmatrix},\mathbf{A}_2(\mathbf{x})=\begin{bmatrix}-0.70 & 0.60\\ 0.40+0.01x_1 & -0.60\end{bmatrix},$$

$$\mathbf{A}_3(\mathbf{x}) = \begin{bmatrix}-0.60 & 0.50+0.01x_1\\ 0.50 & -0.54-0.01x_1\end{bmatrix},$$

$$\mathbf{B}_1(\mathbf{x}) = \begin{bmatrix}0.02+0.01x_1 & 0.10\\ 0.20 & 0.10\end{bmatrix}, \mathbf{B}_2(\mathbf{x}) = \begin{bmatrix}0.12 & 0.10\\ 0.20 & 0.10\end{bmatrix},$$

$$\mathbf{B}_3(\mathbf{x}) = \begin{bmatrix}0.10 & 0.10\\ 0.20-0.01x_1+0.001x_1^2 & 0.10\end{bmatrix},$$

$$\mathbf{C}_1\left(\mathbf{x}\right) = \begin{bmatrix}0.11-0.01x_1 & 0.10\end{bmatrix}, \mathbf{C}_3\left(\mathbf{x}\right) = \begin{bmatrix}0.11 & 0.10\end{bmatrix},$$

$$\mathbf{C}_2\left(\mathbf{x}\right) = \begin{bmatrix}0.11 & 0.1-0.02x_1+0.001x_1^2\end{bmatrix},$$

$$\mathbf{D}_1\left(\mathbf{x}\right) = \begin{bmatrix}0.15+0.01x_1+0.002x_1^2 & 0.15\end{bmatrix},$$

$$\mathbf{D}_2\left(\mathbf{x}\right) = \begin{bmatrix}0.10 & 0.13\end{bmatrix}, \mathbf{D}_3\left(\mathbf{x}\right) = \begin{bmatrix}0.10 & 0.12\end{bmatrix},$$

$$\mathbf{B}_{w2}\left(\mathbf{x}\right) = \begin{bmatrix}0.02 & 0.02\end{bmatrix}, \mathbf{B}_{w3}\left(\mathbf{x}\right) = \begin{bmatrix}0.01 & 0.02\end{bmatrix},$$

$$\mathbf{B}_{w1}\left(\mathbf{x}\right) = \begin{bmatrix}0.01-0.001x_1^2 & 0.02\end{bmatrix}, \mathbf{E}_{w2}\left(\mathbf{x}\right) = \begin{bmatrix}0.02\end{bmatrix},$$

$$\mathbf{E}_{w1}\left(\mathbf{x}\right) = \begin{bmatrix}0.02-0.001x_1^2\end{bmatrix}, \mathbf{E}_{w3}\left(\mathbf{x}\right) = \begin{bmatrix}0.01\end{bmatrix},$$

where the IT2-MFs of PFM are chosen as $\overline{w}_1\left(\mathbf{x}\right) = 1-1/\left(1+e^{-(x_1-4)}\right), \overline{w}_3\left(\mathbf{x}\right) = 1/\left(1+e^{-(x_1-6)}\right), \underline{w}_1\left(\mathbf{x}\right) = 1-1/\left(1+e^{-(x_1-3)}\right), \underline{w}_3\left(\mathbf{x}\right) = 1/\left(1+e^{-(x_1-7)}\right), \overline{w}_2\left(\mathbf{x}\right) = 1-\underline{w}_1\left(\mathbf{x}\right)-\underline{w}_3\left(\mathbf{x}\right), \underline{w}_2\left(\mathbf{x}\right) = 1-\overline{w}_1\left(\mathbf{x}\right)-\overline{w}_3\left(\mathbf{x}\right)$. The embedded type-1 MF is denoted as $\tilde{w}_i(\mathbf{x}) = \underline{\varepsilon}_i(\mathbf{x})\underline{w}_i(\mathbf{x}) + \overline{\varepsilon}_i(\mathbf{x})\overline{w}_i(\mathbf{x})$, the nonlinear type reduction functions are $\underline{\varepsilon}_1(\mathbf{x}) = (\sin(2x_1)+2)/3, \underline{\varepsilon}_3(\mathbf{x}) = (\cos(2x_1)+2)/3$. $\tilde{w}_2(\mathbf{x})$ can obtained by $\tilde{w}_2(\mathbf{x}) = 1-\tilde{w}_1(\mathbf{x})-\tilde{w}_3(\mathbf{x})$. The PDOF controller IT2-MFs with 2 fuzzy rules is selected as $\bar{m}_1\left(\mathbf{y}_c(t_s^u)\right) = e^{-(y_{c1}(t_s^u)-5)^2/12}$, $\underline{m}_1\left(\mathbf{y}_c(t_s^u)\right) = e^{-(y_{c1}(t_s^u)-5)^2/10}$, $\overline{m}_2\left(\mathbf{y}_c(t_s^u)\right) = 1-\underline{m}_1\left(\mathbf{y}_c(t_s^u)\right), \underline{m}_2\left(\mathbf{y}_c(t_s^u)\right) = 1-\overline{m}_1\left(\mathbf{y}_c(t_s^u)\right)$. Similarly, the type reduction functions are $\underline{\kappa}_1(\mathbf{y}_c(t_s^u)) = \underline{\kappa}_2(\mathbf{y}_c(t_s^u)) = 0.5$. To intuitively demonstrate the effectiveness of the IGA-MFD method in approximating multivariable MFs, we set the parameters as population size $P = 30$, $I = 10$, maximum generations $G_{\max} = 1000$, crossover probability $Pcross = 0.6$, mutation probability $Pmuta = 0.01$ and protection probability $mp = 0.1$. Based on these settings,

the corresponding polynomial approximations of the MFs and their approximation errors are obtained.

To verify the effectiveness of the proposed IGA-MFD method (Theorem 3), we present a comparison between the IT2-MFD methods based on the staircase MFs [36](case 2) and the piecewise linear MFs [19] (case 3) in Table I. The two methods are the most representative in the recent IT2-MFD methods. In addition, the PDOF control law based on the MFI method [28] (case 1) is also selected as a control reference for comparison. The controller parameters $\mathbf{O}_{cj}(\mathbf{x}_c)$, $\mathbf{M}_{cij}(\mathbf{x}_c)$, $\mathbf{N}_{cj}(\mathbf{x}_c)$ and the slacked matrices $\mathbf{N}_{g\iota}(\mathbf{x}, \mathbf{x}_c)$ are set to order 2. The slacked matrices $\mathbf{Y}_{ij\iota}(\mathbf{x}, \mathbf{x}_c)$ and $\mathbf{Z}_{ij\iota}(\mathbf{x}, \mathbf{x}_c)$ are set to order 4.

First, we compare the ranges of event-triggered thresholds that different cases could guarantee the stability of the system. The DET parameters are defined as $k_y = 0.1 + 0.1a$ and $k_u = 0.1 + 0.1b$ for the S-C and C-A channels. It should be noted that the settings of the matrix parameters and the threshold parameters are identical to ensure a fair comparison. The stable regions with respect to the event-triggered parameters over the ranges $a = [-1, 4.5], b = [-1, 3]$ are depicted in Fig. 2. As shown in Fig. 2, the proposed IGA-MFD method significantly outperforms the existing MFI in [28] and IT2-MFD in [36] and [19] methods by yielding a larger stable region. This indicates that the IGA-MFD method effectively introduces more information about the IT2-MFs into the stability analysis. Consequently, it significantly extends the allowable set of the DET threshold parameters $k_y$ and $k_u$ to a wider subset of the feasible parameter space, thereby enhancing design flexibility.

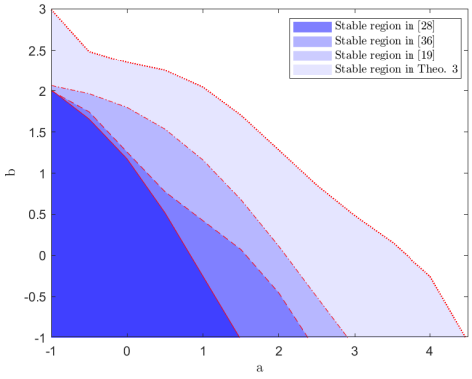


Fig. 2. Comparison of the influence of different cases on the stable region of the DET threshold.

TABLE I
COMPARISON RESULTS OF DIFFERENT CASES

| | Case | Method | $N_y$ | $N_u$ |
|---|---|---|---|---|
| [28] | 1 | MFI | 72 | 75 |
| [36] | 2 | staircase IT2-MFs | 67 | 71 |
| [19] | 3 | piecewise linear IT2-MFs | 61 | 67 |
| Theo. 3 | 4 | IGA-MFD | 60 | 65 |

Next, to improve the reliability of the results, we select the points $a = 3$ and $b = 0.48$ at the boundary of the stable region of Theorem 3 in Fig. 2 for verification with the parameters set as $\alpha_1 = \alpha_2 = 0.99$, $\beta_1 = 0.001$, $\beta_2 = 0.5$, $\sigma_1 = 0.18$, $\sigma_2 = 0.25$, $\omega_{\max} = 1$ and $\rho_{\max} = 0.1$. The PDOF controller gain parameters are shown in Table II. The phase plots under different initial conditions of the state variables $\mathbf{x}(t)$, PDOF controller state variables $\mathbf{x}_c(t)$ under case 4 are shown in Fig. 3 (a)-(b). The trajectories of the PPFS output measurement $y(t)$ and the last transmitted value of the output $\hat{y}(t_p^y)$, PDOF control input $u(t)$ and the last transmitted value of the output $\hat{u}(t_q^u)$, the release intervals of $y(t)$ and $u(t)$ under case 4 are shown in Fig. 4 (a)-(d). The results show that the DET-PDOF controller can stabilize the PPFSs and effectively reduce the frequency of information transmission.

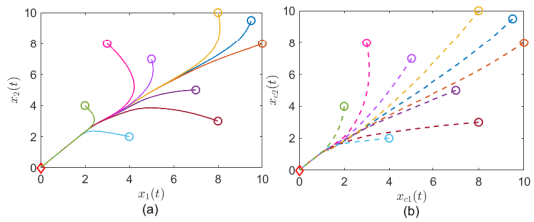


Fig. 3. The simulation results of points $a = 3$ and $b = 0.48$. (a) Phase plots of the state variables $\mathbf{x}(t)$. (b) Phase plots of the state variables $\mathbf{x}_c(t)$.

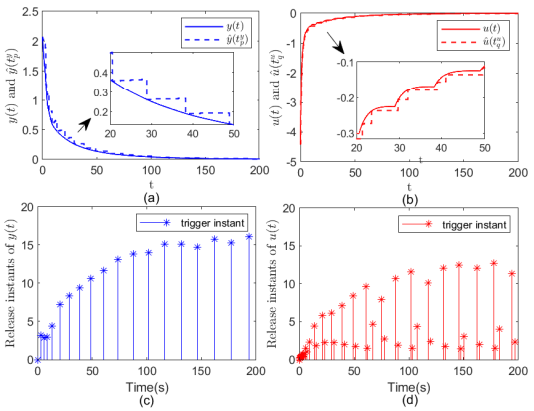


Fig. 4. The simulation results of points $a = 3$ and $b = 0.48$. (a) The trajectories of output $y(t)$ and $\hat{y}(t_p^y)$. (b) The trajectories of input $u(t)$ and $\hat{u}(t_q^u)$. (c) Interevent times of output transmissions. (d) Interevent times of control updates.

To further demonstrate the effect of the presented IGA-MFD approach on DET performance, we compare the number of triggering events $N_y$ and $N_u$ for the dual channels in different cases as shown in Fig. 5 and Fig. 6. The thresholds $k_y \in (0, 1)$ and $k_u \in (0, 1)$ are selected at intervals of 0.05, with all other settings kept identical. Table I summarizes the obtained triggering times of $N_y$ and $N_u$ under different cases where the trigger threshold is $k_y = 0.1$ and $k_u = 0.1$. It is observed that existing methods [28], [36] and [19] fail to yield feasible solutions as the threshold increases and IGA-MFD method proposed in our paper maintains stability over a wider range. Furthermore, the IGA-MFD method can stabilize the PPFSs with fewer event-triggered times under the same thresholds. This performance advantage stems from the IGA-MFD method's ability to utilize IT2-MFs information, leading to fewer data transmissions and optimized network resource utilization compared to existing approaches.

In addition, we conduct a comparative analysis between our

TABLE II
DUAL-EVENT-BASED POLYNOMIAL DYNAMIC OUTPUT-FEEDBACK CONTROL PARAMETERS

| PDOF controller matrices | Event-based PDOF controller parameters |
|---|---|
| PDOF controller system gains $\mathbf{A}_{cij}(\mathbf{x}_c)$ | $\mathbf{A}_{c11}(\mathbf{x}_c) = [-0.0010x_{c1}^2 - 0.0082x_{c1} - 0.8529, -0.0000x_{c1}^2 - 0.0118x_{c1} + 0.2642;$ $0.0004x_{c1}^2 - 0.0140x_{c1} + 0.2760, -0.0002x_{c1}^2 - 0.0096x_{c1} + 0.5991]$; $\mathbf{A}_{c21}(\mathbf{x}_c) = [-0.0009x_{c1}^2 - 0.0009x_{c1} - 0.9828, -0.0000x_{c1}^2 - 0.0099x_{c1} + 0.3417;$ $-0.0002x_{c1}^2 - 0.0067x_{c1} + 0.1856, -0.0012x_{c1}^2 - 0.0037x_{c1} - 0.8098]$; $\mathbf{A}_{c31}(\mathbf{x}_c) = [-0.0001x_{c1}^2 - 0.0085x_{c1} - 0.8473, 0.0002x_{c1}^2 - 0.0072x_{c1} + 0.1653;$ $-0.0001x_{c1}^2 - 0.0084x_{c1} + 0.2884, -0.0021x_{c1}^2 - 0.0031x_{c1} - 0.8857]$; $\mathbf{A}_{c12}(\mathbf{x}_c) = [-0.0011x_{c1}^2 - 0.0066x_{c1} - 0.8396, -0.0004x_{c1}^2 - 0.0076x_{c1} + 0.2618;$ $-0.0001x_{c1}^2 - 0.0111x_{c1} + 0.2920, -0.0006x_{c1}^2 - 0.0064x_{c1} - 0.5979]$; $\mathbf{A}_{c22}(\mathbf{x}_c) = [-0.0015x_{c1}^2 + 0.0023x_{c1} - 0.9745, -0.0007x_{c1}^2 - 0.0062x_{c1} + 0.3638;$ $-0.0005x_{c1}^2 - 0.0043x_{c1} + 0.1945, -0.0019x_{c1}^2 - 0.0008x_{c1} - 0.7970]$; $\mathbf{A}_{c32}(\mathbf{x}_c) = [-0.0006x_{c1}^2 - 0.0035x_{c1} - 0.8506, 0.0001x_{c1}^2 - 0.0020x_{c1} + 0.1520;$ $-0.0005x_{c1}^2 - 0.0048x_{c1} + 0.2896, -0.0025x_{c1}^2 - 0.0032x_{c1} - 0.9470]$. |
| PDOF controller output gains $\mathbf{B}_{cj}(\mathbf{x}_c)$ and $\mathbf{C}_c$ | $\mathbf{B}_{c1}(\mathbf{x}_c) = [0.0013x_{c1}^2 + 0.0289x_{c1} + 1.1821; 0.0011x_{c1}^2 + 0.0254x_{c1} + 0.9027]$; $\mathbf{B}_{c2}(\mathbf{x}_c) = [0.0052x_{c1}^2 - 0.0082x_{c1} + 1.2072; 0.0043x_{c1}^2 - 0.0015x_{c1} + 0.8988]$. $\mathbf{C}_c = [0.2150; 0.2150]$. |
| PDOF controller gains $\mathbf{K}_{cj}(\mathbf{x}, \mathbf{x}_c)$ | $\mathbf{K}_{c1}(\mathbf{x}_c) = [(-0.0085x_{c1}^2 - 0.2119x_{c1} - 5.5070)/\mathbf{M}]$; $\mathbf{K}_{c2}(\mathbf{x}_c) = [(-0.0108x_{c1}^2 - 0.1945x_{c1} - 5.4805)/\mathbf{M}]$. |

[1] $\mathbf{M} = (\boldsymbol{\xi}_1^T + \boldsymbol{\xi}_2^T)\mathbf{B}_{\max}\mathbf{1}_m$, where $\xi_1^T = [18.2864 \quad 22.4810]$ and $\xi_2^T = [2.5300 \quad 3.1878]$.

PDOF control law and the existing T-S fuzzy DOF controller presented in [39]. Fig. 7 shows the evolution of the PDOF controller gains $\mathbf{K}_{cj}(\mathbf{x}_c)$ and T-S fuzzy DOF controller gains $\mathbf{K}_{cj}$. In contrast to the fixed gains in [39], the proposed PDOF gains vary with time, demonstrating higher flexibility. As shown in Figs. 5 and 6, the PDOF scheme achieves fewer triggering times $(N_y, N_u)$ and superior performance under identical thresholds, validating its efficiency.

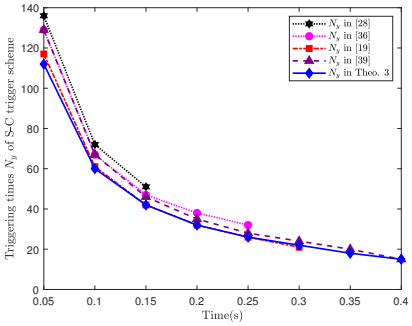


Fig. 5. Comparison of different cases on the triggering times $N_y$ of S-C trigger scheme.

**Example 2.** A system of two-linked tank is borrowed from [40] to illustrate the applicability of the derived results.

$$\begin{cases} \dot{x}_1(t) = u_1(t) - \tilde{R}_1\sqrt{x_1(t)} \\ \qquad -R_{12}\sqrt{|x_1(t) - x_2(t)|}\text{sign}(x_1(t) - x_2(t)) \\ \dot{x}_2(t) = u_2(t) - \tilde{R}_2\sqrt{x_1(t)} \\ \qquad +R_{12}\sqrt{|x_1(t) - x_2(t)|}\text{sign}(x_1(t) - x_2(t)) \end{cases}, \quad (63)$$

where $u_i(t)$ represents the flow of the $i$-th pump, measured in liter/min. $x_i(t)$ holds for the level of $i$-th tank, $i \in 1, 2$. $\tilde{R}_1 = \gamma_1 S_1\sqrt{2g}, \tilde{R}_2 = \gamma_1 S_2\sqrt{2g}, R_{12} = \gamma_{12} S_1\sqrt{2g}$, $\gamma_i$, $\gamma_{ij}$ and $g$ are physical constants, $S_i$ is the tank section. It is assumed that the flow loss coefficient of each water tank is easily affected by various uncertainties, such as manufacturing errors or long-term deformation of parameters like the cross-sectional area and height of the water tank. Meanwhile, some nonlinear behaviors in this system can be represented by partial polynomial terms, such as valve opening degree and flow loss coefficient. Therefore, the system parameters in this paper are given by $\tilde{R}_1(\mathbf{x}) = \tilde{R}_2(\mathbf{x}) = \varpi(0.95 + 0.01x_1(t))$, $R_{12} = 0.52$ and $\varpi \in [\underline{\varpi}, \overline{\varpi}] = [0.92, 1.05]$. Considering the uncertainty parameters in the modeling process, we set $\eta_i(t) =$

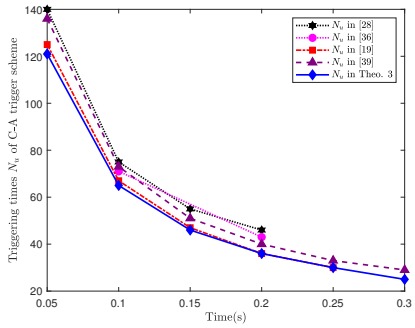


Fig. 6. Comparison of different cases on the triggering times $N_u$ of C-A trigger scheme.

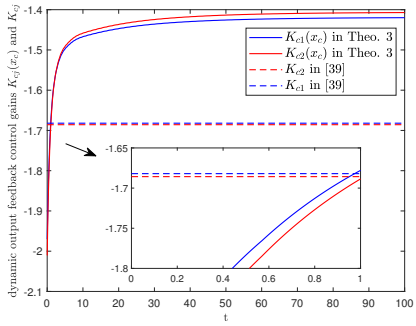


Fig. 7. The evolution of the PFOD controller gains $\mathbf{K}_{cj}(\mathbf{x}_c)$ and T-S fuzzy dynamic output-feedback controller gains $\mathbf{K}_{cj}$.

$\varpi x_i^{-1/2}(t)$ with $\eta_i(t) \in [\underline{\varpi}u_i, \overline{\varpi}v_i] = [\mu_i, \nu_i]$, by the sector nonlinearity technique, we have $\eta_i(t) = \tilde{w}_{i1}(\mathbf{x})\mu_i + \tilde{w}_{i2}(\mathbf{x})\nu_i$, where $\tilde{w}_{i1}(\mathbf{x}) = \frac{\eta_i(t)-\mu_i}{\nu_i-\mu_i}$ and $\tilde{w}_{i2}(\mathbf{x}) = 1 - \tilde{w}_{i1}(\mathbf{x})$, $\nu_i$ and $\mu_i$ represent the maximum and minimum values of $\eta_i(t)$, respectively. Then, the lower and upper MFs are defined as $\overline{w}_{i1}(\mathbf{x}) = \frac{\left(\overline{\varpi}/\sqrt{x_i(t)}\right)-\mu_i}{\nu_i-\mu_i}$, $\underline{w}_{i1}(\mathbf{x}) = \frac{\left(\underline{\varpi}/\sqrt{x_i(t)}\right)-\mu_i}{\nu_i-\mu_i}$, $\overline{w}_{i2}(\mathbf{x}) = 1 - \underline{w}_{i1}(\mathbf{x})$ and $\underline{w}_{i2}(\mathbf{x}) = 1 - \overline{w}_{i1}(\mathbf{x})$.

Next, the dynamics of the two-linked tank system with parameter uncertainties is described by a 4-rule IT2-PFM with

$$\mathbf{A}_1(\mathbf{x}) = \begin{bmatrix} -R_1(\mathbf{x})\mu_1 - \frac{R_{12}\mu_1\mu_2}{\sqrt{|\mu_1{}^2-\mu_2{}^2|}} & \frac{R_{12}\mu_1\mu_2}{\sqrt{|\mu_1{}^2-\mu_2{}^2|}} \\ \frac{R_{12}\mu_1\mu_2}{\sqrt{|\mu_1{}^2-\mu_2{}^2|}} & -R_2(\mathbf{x})\mu_2 - \frac{R_{12}\mu_1\mu_2}{\sqrt{|\mu_1{}^2-\mu_2{}^2|}} \end{bmatrix},$$

$$\mathbf{A}_2(\mathbf{x}) = \begin{bmatrix} -R_1(\mathbf{x})\mu_1 - \frac{R_{12}\mu_1\nu_2}{\sqrt{|\mu_1{}^2-\nu_2{}^2|}} & \frac{R_{12}\mu_1\nu_2}{\sqrt{|\mu_1{}^2-\nu_2{}^2|}} \\ \frac{R_{12}\mu_1\nu_2}{\sqrt{|\mu_1{}^2-\nu_2{}^2|}} & -R_2(\mathbf{x})\nu_2 - \frac{R_{12}\mu_1\nu_2}{\sqrt{|\mu_1{}^2-\nu_2{}^2|}} \end{bmatrix},$$

$$\mathbf{A}_3(\mathbf{x}) = \begin{bmatrix} -R_1(\mathbf{x})\nu_1 - \frac{R_{12}\nu_1\mu_2}{\sqrt{|\nu_1{}^2-\mu_2{}^2|}} & \frac{R_{12}\nu_1\mu_2}{\sqrt{|\nu_1{}^2-\mu_2{}^2|}} \\ \frac{R_{12}\nu_1\mu_2}{\sqrt{|\nu_1{}^2-\mu_2{}^2|}} & -R_2(\mathbf{x})\mu_2 - \frac{R_{12}\nu_1\mu_2}{\sqrt{|\nu_1{}^2-\mu_2{}^2|}} \end{bmatrix},$$

$$\mathbf{A}_4(\mathbf{x}) = \begin{bmatrix} -R_1(\mathbf{x})\nu_1 - \frac{R_{12}\nu_1\nu_2}{\sqrt{|\nu_1{}^2-\nu_2{}^2|}} & \frac{R_{12}\nu_1\nu_2}{\sqrt{|\nu_1{}^2-\nu_2{}^2|}} \\ \frac{R_{12}\nu_1\nu_2}{\sqrt{|\nu_1{}^2-\nu_2{}^2|}} & -R_2(\mathbf{x})\nu_2 - \frac{R_{12}\nu_1\nu_2}{\sqrt{|\nu_1{}^2-\nu_2{}^2|}} \end{bmatrix},$$

$$\mathbf{B}_1 = \mathbf{B}_2 = \mathbf{B}_3 = \mathbf{B}_4 = \mathbf{C}_1 = \mathbf{C}_2 = \mathbf{C}_3 = \mathbf{C}_4 = \begin{bmatrix} 1 & 0 \\ 0 & 1 \end{bmatrix},$$

where $\mathbf{D}_i(\mathbf{x})$, $\mathbf{B}_{wi}(\mathbf{x})$ and $\mathbf{E}_{wi}(\mathbf{x})$ are illustrated in Example 1. The upper and lower MFs of two-linked tank system with 4 fuzzy rules are $\overline{\theta}_{11}(\mathbf{x}) = \overline{w}_{11}(\mathbf{x})\overline{w}_{21}(\mathbf{x}) = \frac{\left(\overline{\varpi}/\sqrt{x_1(t)}\right)-\mu_1}{\nu_1-\mu_1}\frac{\left(\overline{\varpi}/\sqrt{x_2(t)}\right)-\mu_2}{\nu_2-\mu_2}$, $\underline{\theta}_{11}(\mathbf{x}) = \underline{w}_{11}(\mathbf{x})\underline{w}_{21}(\mathbf{x}) = \frac{\left(\underline{\varpi}/\sqrt{x_1(t)}\right)-\mu_1}{\nu_1-\mu_1}\frac{\left(\underline{\varpi}/\sqrt{x_2(t)}\right)-\mu_2}{\nu_2-\mu_2}$, $\overline{\theta}_{21}(\mathbf{x}) = \overline{w}_{21}(\mathbf{x})\overline{w}_{12}(\mathbf{x}) = \frac{\nu_1-\left(\overline{\varpi}/\sqrt{x_1(t)}\right)}{\nu_1-\mu_1}\frac{\left(\overline{\varpi}/\sqrt{x_2(t)}\right)-\mu_2}{\nu_2-\mu_2}$, $\underline{\theta}_{21}(\mathbf{x}) = \underline{w}_{21}(\mathbf{x})\underline{w}_{12}(\mathbf{x}) = \frac{\nu_1-\left(\underline{\varpi}/\sqrt{x_1(t)}\right)}{\nu_1-\mu_1}\frac{\left(\underline{\varpi}/\sqrt{x_2(t)}\right)-\mu_2}{\nu_2-\mu_2}$, $\overline{\theta}_{12}(\mathbf{x}) = \overline{w}_{11}(\mathbf{x})\overline{w}_{22}(\mathbf{x})$, $\underline{\theta}_{12}(\mathbf{x}) = \underline{w}_{11}(\mathbf{x})\bar{w}_{22}(\mathbf{x})$, $\overline{\theta}_{22}(\mathbf{x}) = \overline{w}_{21}(\mathbf{x})\overline{w}_{22}(\mathbf{x})$, $\underline{\theta}_{22}(\mathbf{x}) = \underline{w}_{21}(\mathbf{x})\underline{w}_{22}(\mathbf{x})$. $R_1(\mathbf{x}) = R_2(\mathbf{x}) = 0.95 + 0.01x_1(t)$, $u_1 = 0.22, u_2 = 0.26, v_1 = 0.45, v_2 = 0.41$. The selection of IT2-MFs and type reduction functions of the PDOF controller with 2 fuzzy rules for stabilizing the two-linked tank system is the same as in Example 1.

The initial conditions are set to $\mathbf{x}(0) = [20, 16]$ and $\mathbf{x}_c(0) = [10, 8]$, aiming to track the reference liquid levels $\mathbf{x}_{ref} = [13, 13]$. $k_y$ and $k_u$ are chosen as 0.2 and 0.01. Under the control of the PDOF controller, the trajectories of states $x_i$ and controller states $x_{ci}$, the interevent times of $y(t)$ and $u(t)$ are shown in Fig. 8 (a), (b), (c), and (d), respectively. Fig. 9 (a), (b), (c) and (d) present the trajectories of measurement output $y_i(t)$ and the last transmitted value of output $\hat{y}_i(t_p^y)$, the trajectories of control input $u_i(t)$ and the last transmitted value of input $\hat{u}_i(t_q^u)$, respectively. The results demonstrate that the proposed PDOF controller ensures the stable operation of the two-linked tank system (63), maintaining the liquid levels of the two tanks at their setpoints. The triggering times $N_y$ and $N_u$ are 998 and 44, respectively. This significant reduction in communication effectively reduces system (63) loss and prolongs the equipment's service life.

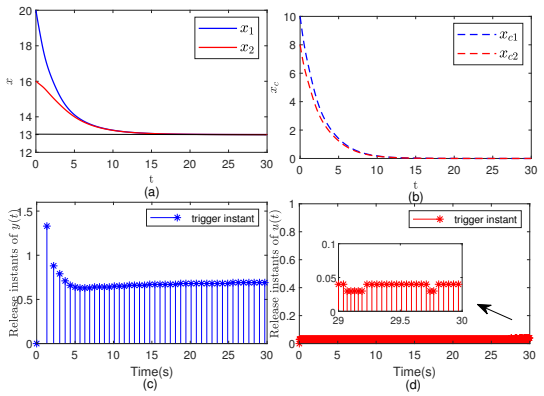


Fig. 8. The simulation results of two-linked tank system. (a) The trajectories of state variables $\mathbf{x}(t)$. (b) The trajectories of state variables $\mathbf{x}_c(t)$. (c) Interevent times of output transmissions. (d) Interevent times of control updates.

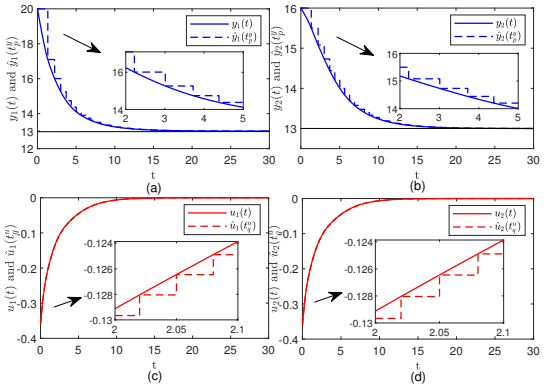


Fig. 9. The simulation results of two-linked tank system. (a)-(b) The trajectories of output $\mathbf{y}(t)$ and $\hat{\mathbf{y}}(t_p^y)$. (c)-(d) The trajectories of control input $\mathbf{u}(t)$ and $\hat{\mathbf{u}}(t_q^u)$.

## VI. Conclusion

This paper presents a design framework for DET-PDOF control of PPFSs under resource constraints. Firstly, a new asynchronous 1-norm DET mechanism is designed for PPFSs to update the system output and PDOF control input, thereby reducing the network burden on the S-C and C-A channels. Then, by utilizing a novel convexification approach and linear copositive Lyapunov analysis, sufficient conditions ensuring system positivity, stability, and $L_1$-gain performance are derived to address the nonconvex problems dependent on polynomial terms. Subsequently, the Chebyshev MFs obtained via the IGA are incorporated into the stability conditions, significantly expanding stable region of DET thresholds and enhancing triggering performance. Finally, numerical and two-linked tank system simulations have verified the effectiveness. In future work, the design of the fuzzy-rule-dependent event-triggered schemes, online MF optimization policies, the application of observer-based feedback and tracking controllers in PNS will be addressed.

## References

[1] A. Aleksandrov, "On the existence of diagonal Lyapunov-Krasovskii functionals for a class of nonlinear positive time-delay systems," *Automatica*, vol. 160, p. 111449, 2024.

[2] L. Wang, B. Zheng, X. Xie, and H. K. Lam, "New stability criterion for positive impulsive fuzzy systems by applying polynomial impulse-time-dependent method," *IEEE Transactions on Cybernetics*, vol. 54, no. 9, pp. 5473–5482, 2024.

[3] X. Li, X. Wang, F. Liu, H. K. Lam, and Y. Du, "Stability analysis and event-triggered control for IT2 discrete-time positive polynomial fuzzy networked control systems with time delay," *IEEE Transactions on Fuzzy Systems*, vol. 32, no. 3, pp. 1346–1358, 2024.

[4] M. Han, H. K. Lam, F. Liu, Y. Tang, B. Han, and H. Zhou, "Stabilization analysis and impulsive controller design for positive interval type-2 polynomial fuzzy systems," *IEEE Transactions on Fuzzy Systems*, vol. 30, no. 9, pp. 3952–3966, 2022.

[5] X. Li, Y. Shan, H. K. Lam, Z. Bao, and J. Zhao, "Exponential stabilization of polynomial fuzzy positive switched systems with time delay considering MDADT switching signal," *IEEE Transactions on Fuzzy Systems*, vol. 32, no. 1, pp. 174–187, 2024.

[6] L. Farina and S. Rinaldi, "Positive linear systems: theory and applications," *journal of veterinary medical science*, 2000.

[7] N. H. Sau and M. V. Thuan, "Event-triggered control for linear positive discrete-time singular systems with time delay," *IEEE Transactions on Systems, Man, and Cybernetics: Systems*, vol. 55, no. 11, pp. 8625–8637, 2025.

[8] J. Zhang, G. Zheng, Y. Feng, and Y. Chen, "Event-triggered state-feedback and dynamic output-feedback control of PMJSs with intermittent faults," *IEEE Transactions on Automatic Control*, vol. 68, no. 2, pp. 1039–1046, 2023.

[9] W. Chen, F. Deng, G. Zong, X. Wang, and Z. Ma, "A zonotope-based event-triggered control approach for asynchronously switched positive systems," *IEEE Transactions on Cybernetics*, vol. 55, no. 12, pp. 5650–5660, 2025.

[10] J. Cheng, Y. Wu, Z. G. Wu, and H. Yan, "Nonstationary filtering for fuzzy markov switching affine systems with quantization effects and deception attacks," *IEEE Transactions on Systems, Man, and Cybernetics: Systems*, vol. 52, no. 10, pp. 6545–6554, 2022.

[11] W. Xie, G. Chen, W. Wu, and Y. Peng, "Functional observer design for T-S fuzzy systems with complex unmeasurable premise variables," *IEEE Transactions on Cybernetics*, 2025, doi:10.1109/TCYB.2025.3624426.

[12] X. Li, K. Mehran, and Z. Bao, "Membership function, time delay-dependent $\eta$-exponential stabilization of the positive discrete-time polynomial fuzzy model control system," *IEEE Transactions on Fuzzy Systems*, vol. 30, no. 7, pp. 2197–2209, 2022.

[13] S. H. Tsai, W. H. Lee, K. Tanaka, Y. J. Chen, and H. K. Lam, "Polynomial fuzzy observer-based feedback control for nonlinear hyperbolic PDEs systems," *IEEE Transactions on Cybernetics*, vol. 54, no. 9, pp. 5257–5269, 2024.

[14] J. Ding, Y. Liu, J. Yu, and X. Yang, "Dissipativity-based integrated fault estimation and fault tolerant control for IT2 polynomial fuzzy systems with sensor and actuator faults," *IEEE Transactions on Fuzzy Systems*, vol. 31, no. 9, pp. 2956–2965, 2023.

[15] Y. Zhao, L. Wang, Q. Wang, and H. K. Lam, "Stability and stabilization of positive fuzzy systems via polynomial lyapunov functions with application to tank level control," *IEEE Transactions on Automation Science and Engineering*, vol. 22, pp. 22 102–22 111, 2025.

[16] P. S. Amartya, S. Kabir, S. C. K. Babu and M. Jahan, "An interval creation approach to construct interval type-2 fuzzy sets," in *2024 IEEE International Conference on Fuzzy Systems (FUZZ-IEEE)*, 2024, pp. 1–9.

[17] D. Wang, and S. Xu, "Disturbance observer-based $H_\infty$ control for interval type-2 fuzzy hidden markov jump systems subject to deception attacks," *IEEE Transactions on Cybernetics*, vol. 54, no. 10, pp. 5843–5851, 2024.

[18] J. Sun, K. Ma, and Y. Feng, "A dynamic interval type-2 fuzzy stochastic configuration network for nonlinear system modeling," *IEEE Transactions on Fuzzy Systems*, vol. 33, no. 10, pp. 3609–3623, 2025.

[19] M. Han, G. Guo, H. K. Lam, B. Han, and Z. Wang, "Event-triggered positive filter design for positive polynomial fuzzy systems via premise integration and membership-function-dependent methods," *IEEE Transactions on Fuzzy Systems*, vol. 31, no. 11, pp. 3799–3811, 2023.

[20] J. Cheng, J. H. Park, Z. G. Wu, and H. Yan, "Ultimate boundedness control for networked singularly perturbed systems with deception attacks: A markovian communication protocol approach," *IEEE Transactions on Network Science and Engineering*, vol. 9, no. 2, pp. 445–456, 2022.

[21] K. Xie, Y. Zheng, Y. Jiang, W. Lan, and X. Yu, "Optimal dynamic output feedback control of unknown linear continuous-time systems by adaptive dynamic programming," *Automatica*, vol. 163, p. 111601, 2024.

[22] J. Wu, M. Lu, F. Deng, and J. Chen, "Robust output regulation of linear uncertain systems by dynamic event-triggered output feedback control," *IEEE Transactions on Cybernetics*, vol. 53, no. 11, pp. 7333–7341, 2023.

[23] N. Zhao, D. Lun, H. Zhang, X. Zhao, and I. J. Rudas, "Composite anti-disturbance control for networked systems with disturbances and actuator attacks via event-triggered output feedback," *IEEE Transactions on Cybernetics*, 2025, doi:10.1109/TCYB.2025.3609819.

[24] A. Meng, H. K. Lam, Y. Yu, X. Li, and F. Liu, "Static output feedback stabilization of positive polynomial fuzzy systems," *IEEE Transactions on Fuzzy Systems*, vol. 26, no. 3, pp. 1600–1612, 2018.

[25] A. Meng, H. K. Lam, Z. Wang, and F. Liu, "Static output feedback fault tolerant control and relaxed stability analysis of positive polynomial fuzzy systems," *IEEE Transactions on Fuzzy Systems*, vol. 30, no. 9, pp. 3928–3939, 2022.

[26] J. Wang, J. Liang, and J. Yang, "Nonfragile dynamic output-feedback control for positive singular systems under the switched mechanism and round-robin protocol," *Nonlinear Analysis: Hybrid Systems*, vol. 47, p. 101292, 2023.

[27] H. Y. Sun, S. Hou, S. Du, H. G. Han, and J. F. Qiao, "Sampled-data $H_\infty$ dynamic output-feedback control for NCSs with successive packet losses and stochastic sampling," *IEEE Transactions on Cybernetics*, vol. 54, no. 10, pp. 6024–6034, 2024.

[28] H. Zhang, N. Zhao, S. Wang, and R. K. Agarwal, "Improved event-triggered dynamic output feedback control for networked T-S fuzzy systems with actuator failure and deception attacks," *IEEE Transactions on Cybernetics*, vol. 53, no. 12, pp. 7989–7999, 2023.

[29] D. Liang and J. Huang, "Robust output regulation of linear systems by event-triggered dynamic output feedback control," *IEEE Transactions on Automatic Control*, vol. 66, no. 5, pp. 2415–2422, 2021.

[30] Z. Liu, Y. Sun, and S. Ma, "Event-triggered dynamic output feedback control for switched singular systems with asynchronous switching," *IEEE Transactions on Automation Science and Engineering*, vol. 22, pp. 16 287–16 296, 2025.

[31] Y. Ma, and W. Che, "Dynamic event-triggered output feedback separation design for networked control systems," *IEEE Transactions on Cybernetics*, vol. 55, no. 8, pp. 3788–3798, 2025.

[32] Z. Sheng and S. Xu, "An aperiodic-sampling-dependent event-triggered control strategy for interval type-2 fuzzy systems: New communication scheme and discontinuous functional," *IEEE Transactions on Cybernetics*, vol. 54, no. 11, pp. 6436–6447, 2024.

[33] Q. Hou and J. Dong, "Cooperative fault-tolerant output regulation of linear heterogeneous multiagent systems via an adaptive dynamic event-triggered mechanism," *IEEE Transactions on Cybernetics*, vol. 53, no. 8, pp. 5299–5310, 2023.

[34] Y. Liu, X. Xie, R. M. Palhares, and J. Sun, "Dual channels event-triggered asymptotic consensus control for fractional-order nonlinear multiagent systems," *IEEE Transactions on Cybernetics*, vol. 54, no. 11, pp. 6780–6791, 2024.

[35] Z. Wang, H. K. Lam, A. Meng, and Z. Li, "Relaxed stabilization of event-triggered interval type-2 T-S fuzzy positive systems with stochastic actuator failure," *IEEE Transactions on Fuzzy Systems*, vol. 31, no. 12, pp. 4435–4446, 2023.

[36] Y. Zeng, H. K. Lam, B. Xiao, and L. Wu, "$L_2$-$L_\infty$ control of discrete-time state-delay interval type-2 fuzzy systems via dynamic output feedback," *IEEE Transactions on Cybernetics*, vol. 52, no. 6, pp. 4198–4208, 2022.

[37] H. Zhou, H. K. Lam, B. Xiao, and C. Xuan, "Integrated fault-tolerant control design with sampled-output measurements for interval type-2 Takagi-Sugeno fuzzy systems," *IEEE Transactions on Cybernetics*, vol. 54, no. 9, pp. 5068–5077, 2024.

[38] Z. Bao, X. Li, H. K. Lam, Y. Peng, and F. Liu, "Membership-function-dependent stability analysis for polynomial-fuzzy-model-based control systems via Chebyshev membership functions," *IEEE Transactions on Fuzzy Systems*, vol. 29, no. 11, pp. 3280–3292, 2021.

[39] E. S. Tognetti and T. M. Linhares, "Dynamic output feedback controller design for uncertain Takagi-Sugeno fuzzy systems: A premise variable selection approach," *IEEE Transactions on Fuzzy Systems*, vol. 29, no. 6, pp. 1590–1600, 2021.

[40] Z. Bao and X. Li, "Relaxed event-triggered tracking control of positive T-S fuzzy systems via a membership function method," *ISA Transactions*, vol. 157, pp. 78–88, 2025.